

# Unearthing the soil C cycle with DNA-SIP

Charles Pepe-Ranney and Ashley N Campbell \* †, Chantal Koechli \* , Sean Berthrong, and Daniel H Buckley \* ‡

\* These authors contributed equally to the manuscript and should be considered co-first authors, †School of Integrative Plant Sciences, Cornell University, New York, USA, and ‡corresponding author

Submitted to Proceedings of the National Academy of Sciences of the United States of America

## Abstract

We explored the dynamics of microbial carbon (C) decomposition in soil by coupling DNA Stable Isotope Probing (SIP) and high throughput sequencing. Our experiment evaluated the degradative succession hypothesis, described dynamics of C metabolism during organic matter degradation, and characterized bacteria that metabolize labile and structural C in soils. We added a complex amendment representing plant derived organic matter to soil substituting  $^{13}\text{C}$ -xylose or  $^{13}\text{C}$ -cellulose for unlabeled equivalents in two experimental treatments. Xylose and cellulose are abundant components in plant biomass and represent labile and structural C pools, respectively. We assessed  $^{13}\text{C}$  assimilation into DNA for SSU rRNA gene OTUs finding evidence of  $^{13}\text{C}$ -incorporation from  $^{13}\text{C}$ -xylose and  $^{13}\text{C}$ -cellulose in 49 and 63 OTUs, respectively. Microorganisms primarily assimilated xylose-C into DNA on days 1, 3, and 7 and cellulose-C on days 14 and 30. The types of microorganisms that assimilated xylose-C changed with time initially dominated by *Firmicutes* at day 1 followed by *Bacteroidetes* at day 3 and then *Actinobacteria* at day 7. Temporal dynamics of  $^{13}\text{C}$ -labeling suggests  $^{13}\text{C}$  microorganisms at different trophic levels exchanged C. Microbes that metabolized cellulose-C belonged to cosmopolitan soil lineages that remain uncharacterized physiologically, including: *Spartobacteria*, *Chloroflexi* and *Planctomycetes*. Our study unearths links microorganisms to specific soil C processes revealing ecological properties of specific microorganisms within complex communities.

stable isotope probing | structure-function relationships | soil microbial ecology | 16S rRNA gene

Abbreviations: C, Carbon; OTU, Operational Taxonomic Unit; SOM, Soil Organic Matter; BD, Buoyancy Density; SIP, Stable Isotope Probing

## Significance

Soil microorganisms drive C flux through the terrestrial biosphere, and while accounting for microbial physiological diversity improves global C mod-

els, characterizing the ecophysiology of microbes involved with C decomposition has proven difficult due to their overwhelming diversity. We characterized C use of individual microbes in soil and show different C forms have distinct decomposition dynamics governed by different microbial lineages. For example, we found microbes belonging to poorly characterized but cosmopolitan taxa in soils assimilated cellulose C into DNA. These microbes may drive cellulose decomposition on a global scale. We identify microbial lineages engaging in labile and structural C decomposition and explore their ecological properties.

## Introduction

Soils worldwide contain 2,300 Pg of carbon (C) which accounts for nearly 80% of the C present in the terrestrial biosphere [1, 2]. C respiration by soil microorganisms produces annually tenfold more CO<sub>2</sub> than fossil fuel emissions [3]. Despite the contribution of microorganisms to global C flux, many global C models ignore microbial physiological diversity and its impacts on microbial activity in soils. [4–6]. Further, predictions of climate change feedbacks on soil C flux improve when geochemical models explicitly represent microbial physiology [7]. However, we still know little about the ecophysiology of soil microorganisms, and such knowledge should assist the development and refinement of global C models [8–10].

Cellulose comprises most plant C (30–50%) followed by hemicellulose (20–40%), and lignin (15–25%) [11]. Hemicellulose, being the most soluble,

## Reserved for Publication Footnotes

degrades in the early stages of decomposition. Xylans are often an abundant component of hemicellulose, and xylans themselves include differing amounts of xylose, glucose, arabinose, galactose, mannose, and rhamnose [12]. Xylose is often the most abundant sugar in hemicellulose, comprising as much as 60–90% of xylan in some plants (e.g. hardwoods) [?], wheat [14], and switchgrass [15]. Microbes that respire sugars proliferate during the initial stages of decomposition [16, 17], and metabolize as much as 75% of sugar C during the first 5 days of decomposition [18]. In contrast, cellulose decomposition proceeds more slowly with rates increasing for approximately 15 days while degradation continues for 30–90 days [18, 19]. It is hypothesized that different microbial guilds mediate the decomposition of different plant biomass components [19, 20, 22?]. For instance, this degradative succession hypothesis posits that fast growing organisms proliferate in response to the labile fraction of plant biomass such as sugars [23, 24] followed by slow growing organisms targeting structural C such as cellulose [23]. Evidence to support the degradative succession hypothesis comes from observing soil respiration dynamics and characterizing microbes cultured at different stages of decomposition. The degree to which the succession hypothesis presents an accurate model of litter decomposition has been called into question [25? , 26] and it’s clear that we need new approaches to dissect microbial contributions to C transformations in soils.

Though microorganisms mediate 80–90% of the soil C-cycle [27, 28], and microbial community composition can account for significant variation in C mineralization [29], terrestrial C-cycle models rarely consider the community composition of soils [30, 31]. We measure rates of soil C transformations without knowledge of the organisms that mediate these reactions [28], leaving undefined the importance of community membership towards maintaining ecosystem function [28, 32, 33]. Variation in microbial community composition can be linked effectively to rates of soil processes when diagnostic genes for specific functions are available (e.g. denitrification [34], nitrification [35–37], methanotrophy [38], and nitrogen fixation [39]). However, the complexity of soil C transformations and the lack of diagnostic genes for describing these transformations has limited progress in characterizing the contributions of individual microbes to the soil C-cycle. Remarkably, we still lack basic information on the physiology and ecology of the majority of organisms that live in soils. For example, contributions to soil processes remain uncharacterized for entire and cosmopolitan bacterial phyla in soil such as *Acidobacteria*, *Chloroflexi*, *Planctomycetes*, and *Verrucomicrobia*. These phyla combined can

comprise 32% of soil microbial communities (based on surveys of the SSU rRNA genes in soil) [40? ].

Characterizing the functions of microbial taxa has relied historically on culturing microorganisms and subsequently characterizing physiology in the laboratory and on environmental surveys or genes diagnostic for specific processes. However, most microorganisms are difficult to grow in culture [40] and many processes lack suitable diagnostic genes. Nucleic acid stable-isotope probing (SIP) links genetic identity and activity without the need to grow microorganisms in culture and has expanded our knowledge of microbial contributions to biogeochemical processes [42]. However, nucleic acid SIP has notable complications including the need to add large amounts of labeled substrate [43], label dilution resulting in partial labelling of nucleic acids [43–45], the potential for cross-feeding and secondary label incorporation [45–50], and variation in genome G+C content [51–54]. As a result, most applications of SIP have targeted specialized microorganisms such as methanotrophs [43], methanogens [55], syntrophs [56], or microbes that target pollutants [57]. SIP has proved less useful for exploring the soil C-cycle because it has lacked the resolution necessary to manage effectively the signal complexity that results from adding components of plant biomass to microbial communities in soil. High throughput DNA sequencing technology, however, improves the resolving power of SIP [58].

Coupling SIP with high throughput DNA sequencing now enables exploration of microbial C-cycling in soils. SSU rRNA amplicons can be sequenced from numerous density gradient fractions across multiple samples thereby increasing the resolution of a typical nucleic acid SIP experiment [59]. It is now possible to use far less isotopically labeled substrate resulting in more environmentally realistic experimental conditions [58]. We have employed such a high resolution DNA stable isotope probing approach to explore the assimilation of <sup>13</sup>C labeled xylose and/or cellulose into bacterial DNA in an agricultural soil.

Specifically, we added to soil a complex amendment that simulated organic matter derived from fresh plant biomass. All treatments received the same amendment but the identity of the isotopically labeled substrate was varied between treatments. We set up a control treatment where all components were unlabeled, a treatment with <sup>13</sup>C-xylose, and a treatment with <sup>13</sup>C-cellulose. Soil was sampled at days 1, 3, 7, 14, and 30 and we identified the microorganisms had assimilated <sup>13</sup>C into DNA at each point in time. The experiment was designed to provide a test of the degradative succession hypothesis in the context of soil bacteria, to identify soil bacteria that metabolize xylose

and cellulose, and to characterize temporal dynamics of xylose and cellulose metabolism in soil.

## Results

After adding an organic matter amendment to soil, we tracked the flow of C from xylose or cellulose into microbial DNA over time using DNA-SIP (Figure S1). The amendment consisted of various plant biomass compounds including cellulose, lignin, sugars found in hemicellulose, amino acids, and inorganic salts (see Supplemental Methods). The amendment was added at 2.3 mg C g<sup>-1</sup> soil dry weight (d.w.), and this comprised 16% of the total C in the soil. The cellulose-C (0.88 mg C g<sup>-1</sup> soil d.w.) and xylose-C (0.42 mg C g<sup>-1</sup> soil d.w.) in the amendment comprised 6% and 3% of the total C in the soil, respectively. The soil microbial community respired 65% of the xylose within one day and 29% of the added xylose remained in the soil at day 30 (Figure S2). In contrast, cellulose-C declined at a constant rate of approximately 18 µg C d<sup>-1</sup> g<sup>-1</sup> soil d.w. and 40% of added cellulose-C remained in the soil at day 30 (Figure S2).

**13C-labeling of OTUs changed with time and substrate.** We assessed assimilation of <sup>13</sup>C into microbial DNA by comparing the SSU rRNA gene sequence composition of SIP density gradient fractions from <sup>13</sup>C treatments to control. All treatments used the same amendment which included xylose and cellulose, but <sup>13</sup>C-xylose or <sup>13</sup>C-cellulose was substituted for its unlabeled equivalent in two amendments. A treatment without isotopically labeled components served as the “control”. In the gradient density fractions of the control, fraction density represented the majority of the variance in SSU rRNA gene composition (Figure 1). DNA buoyant density correlates with G+C content [51] and therefore DNA G+C content influences variation in the SSU rRNA gene composition of density gradient fractions. For the <sup>13</sup>C-cellulose treatment, SSU rRNA gene composition in gradient fractions deviated from control at high density (> 1.72 g mL<sup>-1</sup>) on days 14 and 30 (Figure 1). For the <sup>13</sup>C-xylose treatment, SSU rRNA gene composition in density gradient fractions also deviated from control in high density fractions, but in contrast to the <sup>13</sup>C-cellulose treatment it deviated from control on days 1, 3, and 7 (Figure 1). SSU rRNA gene composition from <sup>13</sup>C-cellulose treatment and <sup>13</sup>C-xylose treatment density fractions differed at high density indicating different microorganisms assimilated C from xylose than cellulose (Figure 1). Further, in the <sup>13</sup>C-cellulose treatment, the SSU rRNA gene sequence composition of high density fractions at days 14 and 30 was similar indicating similar microorganisms had <sup>13</sup>C

labeled DNA in <sup>13</sup>C-cellulose treatments at days 14 and 30. In contrast, in the <sup>13</sup>C-xylose treatment, the SSU rRNA gene composition high density fractions varied between days 1, 3, and 7 indicating that different microbes had <sup>13</sup>C labeled DNA on these days. In the <sup>13</sup>C-xylose treatment, the SSU gene composition of high density fractions was similar to control on days 14 and 30 (Figure 1) indicating that <sup>13</sup>C was no longer detectable on these days for this treatment.

## Temporal dynamics DNA <sup>13</sup>C incorporation of OTUs.

We monitored the soil microcosm microbial community over the course of the experiment by surveying SSU rRNA genes in non-fractionated DNA from the soil microcosms. The SSU rRNA gene composition of the non-fractionated DNA changed with time (Figure S3, P-value = 0.023, R<sup>2</sup> = 0.63, Adonis test [60]). In contrast, the community showed no statistical evidence for changing with treatment (P-value was 0.23) (Figure S3). The latter result demonstrates the substitution of <sup>13</sup>C-labeled substrates for unlabeled equivalents could not be shown to alter community composition. Twenty-nine OTUs exhibited sufficient statistical evidence (adjusted P-value < 0.10) to conclude they changed in relative abundance over the course of the experiment (Figure S4). When SSU rRNA gene abundances were combined at the taxonomic rank of “class”, the classes that changed in abundance (P-value < 0.10) were the *Bacilli* (decreased), *Flavobacteria* (decreased), *Gammaproteobacteria* (decreased), and *Herpetosiphonales* (increased) (Figure S5). Of the 29 OTUs that changed in relative abundance over time, 14 putatively incorporated <sup>13</sup>C into DNA (Figure S4). OTUs that likely assimilated <sup>13</sup>C from <sup>13</sup>C-cellulose into DNA tended to increase in relative abundance with time whereas OTUs that assimilated <sup>13</sup>C from <sup>13</sup>C-xylose tended to decrease (Figure S6). Those OTUs that responded to both substrates did not exhibit a consistent relative abundance response over time as a group (Figure S4 and S6).

## OTUs that assimilated <sup>13</sup>C into DNA.

If an OTU exhibited strong evidence for assimilating <sup>13</sup>C into DNA, we refer to that OTU as a “responder” (see Supplemental Methods for our operational definition of “responder”). The SSU rRNA gene sequences produced in this study could be distributed into 5,940 OTUs and we assessed the evidence of <sup>13</sup>C incorporation into DNA from <sup>13</sup>C-cellulose and <sup>13</sup>C-xylose for each OTU. Forty-one OTUs responded to <sup>13</sup>C-xylose, 55 OTUs responded to <sup>13</sup>C-cellulose, and 8 OTUs responded to both xylose and cellulose (Figure S7, Figure 2, Figure 3, Table S1, and Table S2). The number

<sup>310</sup> of xylose responders peaked at days 1 and 3 and declined with time. In contrast, the number of cellulose responders increased with time peaking at <sup>370</sup> days 14 and 30 (Figure S8).

The phylogenetic composition of xylose responders changed with time and the majority (86%) of xylose responders shared > 97% SSU rRNA gene sequence identity with bacteria cultured in isolation (Figure 2 and 4). On day 1, *Bacilli* OTUs represented 84% of xylose responders and the majority of these OTUs were closely related to cultured representatives of the genus *Paenibacillus* (Table S2). For example, “OTU.57” (Table S2), annotated as *Paenibacillus*, had a strong signal of <sup>13</sup>C assimilation from <sup>13</sup>C-xylose into DNA at <sup>325</sup> day 1 coinciding with its maximum relative abundance in non-fractionated DNA. The relative abundance of “OTU.57” declined until day 14 and did not appear to be <sup>13</sup>C labeled after day 1 (Figure S9). On day 3, *Bacteroidetes* OTUs comprised 63% of xylose responders (Figure 4) and these OTUs were closely related to cultured representatives of the *Flavobacteriales* and *Sphingobacteriales* (Table S2). For example, “OTU.14”, annotated as a Flavobacterium, had a strong signal for <sup>13</sup>C labeling in the <sup>13</sup>C-xylose treatment at <sup>335</sup> days 1 and 3 coinciding with its maximum relative abundance in non-fractionated DNA. The relative abundance of “OTU.14” then declined until day 14 and did not show evidence of <sup>13</sup>C labeling beyond day 3 (Figure S9). Finally, on day 7, *Actinobacteria* OTUs represented 53% of the xylose responders and these OTUs were closely related to cultured representatives of *Micrococcales* (Table S2, Figure 3). For example, “OTU.4”, annotated as *Agromyces*, had signal of <sup>13</sup>C labeling in the <sup>13</sup>C-xylose treatment on days 1, 3 and 7 with the strongest evidence of <sup>13</sup>C labeling at day 7 and did not appear <sup>13</sup>C labeled at days 14 and 30. “OTU.4” relative abundance in non-fractionated <sup>350</sup> DNA increased until day 3 and then declined until day 30 (Figure S9). *Proteobacteria* were also common among xylose responders at day 7 where they comprised 40% of xylose responder OTUs. Notably, *Proteobacteria* represented the majority (<sup>355</sup> of 8) of OTUs that responded to both cellulose and xylose (Figure S7).

The phylogenetic composition of cellulose responders did not change with time unlike the phylogenetic composition of xylose responders. Also, <sup>360</sup> in contrast to xylose responders, cellulose responders often were not closely related (< 97% SSU rRNA gene sequence identity) to cultured isolates. Both the relative abundance and the number of cellulose responders increased over time <sup>365</sup> peaking at days 14 and 30 (Figures 2, S8, and S6). Cellulose responders belonged to the *Proteobacteria* (46%), *Verrucomicrobia* (16%), *Plan-*

*tomycetes* (16%), *Chloroflexi* (8%), *Bacteroidetes* (8%), *Actinobacteria* (3%), and *Melanobacteriia* (1 <sup>370</sup> OTU) (Table S1). The majority (86%) of cellulose responders in the *Proteobacteria* were closely related (> 97% identity) to bacteria already cultured in isolation, including representatives of the genera: *Cellvibrio*, *Devosia*, *Rhizobium*, and *Sorangium*, which are all known for their ability to degrade cellulose (Table S1). Proteobacterial cellulose responders belonged to *Alpha-* (13 OTUs), *Beta-* (4 OTUs), *Gamma-* (5 OTUs), and *Deltaproteobacteria* (6 OTUs).

The majority (85%) of cellulose responders outside of the *Proteobacteria* shared < 97% SSU rRNA gene sequence identity to bacteria cultured in isolation. For example, most (70%) of the *Verrucomicrobia* cellulose responders fell within unidentified *Spartobacteriia* clades (Figure ??), and these shared < 85% SSU rRNA gene sequence identity to any characterized isolate. The *Spartobacteriia* OTU “OTU.2192” exemplified many cellulose responders (Figure ??, Table S1). “OTU.2192” increased in non-fractionated DNA relative abundance with time and evidence for <sup>13</sup>C labeling of “OTU.2192” in the <sup>13</sup>C-cellulose treatment increased over time with the strongest evidence at <sup>385</sup> days 14 and 30 (Figure S9). Most *Chloroflexi* cellulose responders belonged to an unidentified clade within the *Herpetosiphonales* and they shared < 89% SSU rRNA gene sequence identity to any characterized isolate. Characteristic of *Chloroflexi* cellulose responders, “OTU.64” increased in relative <sup>390</sup> abundance over 30 days and evidence for <sup>13</sup>C labeling of “OTU.64” in the <sup>13</sup>C-cellulose treatment peaked days 14 and 30 (Figure S9). Cellulose responders found within the *Bacteroidetes* fell within the *Cytophagales* contrasting with *Bacteroidetes* xylose responders that fell instead within the *Flavobacteriales* or *Sphingobacteriales* (Figure ??). *Bacteroidetes* cellulose responders included one OTU that shared 100% SSU rRNA gene sequence identity to species of *Sporocytophaga*, a genus that <sup>405</sup> includes known cellulose degraders.

### Characteristics of cellulose and xylose responders.

Cellulose responders, relative to xylose responders, tended to have lower relative abundance in non-fractionated DNA, demonstrated signal consistent with higher atom % <sup>13</sup>C in labeled DNA, and had lower estimated *rrn* copy number (Figure 5). In the non-fractionated DNA, cellulose responders had lower relative abundance ( $7e^{-4}$  (s.d.  $2e^{-3}$ )) than xylose responders ( $2e^{-3}$  (s.d.  $4e^{-3}$ )) (Figure 4, P-value = 0.00028, Wilcoxon Rank Sum test). Six of the ten most common OTUs observed in the non-fractionated DNA responded to xylose, and, eight of the ten most abundant responders <sup>410</sup>

to xylose or cellulose in the non-fractionated DNA  
425 were xylose responders.

DNA buoyant density (BD) increases in proportion to the atom %  $^{13}\text{C}$  of the DNA. Hence, the extent of  $^{13}\text{C}$  incorporation into DNA can be evaluated as by the difference in BD between  
430  $^{13}\text{C}$ -labeled and unlabeled DNA. We calculated for each OTU its mean BD weighted by relative abundance to determine its center of mass within a given density gradient. We then quantified for each OTU the difference in center of mass between  
435 control gradients and gradients from  $^{13}\text{C}$ -xylose or  $^{13}\text{C}$ -cellulose treatments (see supplemental methods for the detailed calculation). We refer to the change in center of mass position for an OTU in response to  $^{13}\text{C}$  labeling as  $\Delta\hat{BD}$ .  $\Delta\hat{BD}$  can be  
440 used to compare relative differences in  $^{13}\text{C}$  labeling between OTUs.  $\Delta\hat{BD}$  values, however, are not comparable to the BD changes observed for DNA from pure cultures which generate molecules uniform in isotopic labeling, in part because  $\Delta\hat{BD}$   
445 is based on relative abundance in density gradient fractions (and not DNA concentration) and in part because all members of an OTU may not uniformly respond to the isotopic label. Cellulose responder  
450  $\Delta\hat{BD}$  ( $0.0163 \text{ g mL}^{-1}$  (s.d.  $0.0094$ )) was greater than that of xylose responders ( $0.0097 \text{ g mL}^{-1}$  (s.d.  $0.0094$ )) (Figure 5, P-value =  $1.8610\text{e}^{-6}$ , Wilcoxon Rank Sum test).

We predicted the *rrn* gene copy number for responders as described [61]. The number of *rrn* gene  
455 copies a microorganism has is correlated to its ability to proliferate in response to rapid nutrient influx [62]. Cellulose responders possessed fewer estimated *rrn* copy numbers ( $2.7$  ( $1.2$  s.d.)) than xylose responders ( $6.2$  ( $3.4$  s.d.)) (Figures 5 and S10; P =  
460  $1.878\text{e}^{-9}$ ). Furthermore, the estimated *rrn* gene copy number for xylose responders was inversely related to the day of first response (P =  $2.02\text{e}^{-15}$ , Figure S10, Figure 5).

We assessed phylogenetic clustering of  $^{13}\text{C}$ -responsive OTUs with the Nearest Taxon Index (NTI) and the Net Relatedness Index (NRI) [63]. We also quantified the average clade depth of cellulose and xylose responders with the consenTRAIT metric [64]. Briefly, the NRI and NTI evaluate  
470 phylogenetic clustering against a null model for the distribution of a trait in a phylogeny. The NRI and NTI values are z-scores or standard deviations from the mean and thus the greater the magnitude of the NRI/NTI, the stronger the evidence for clustering (positive values) or overdispersion (negative values). NRI assesses overall clustering whereas the NTI assesses terminal clustering. An NRI of  $1.96$ , for instance, would signify overall phylogenetic clustering with a corresponding P-value of  
475  $0.05$  [65]. The consenTRAIT metric is a measure of the average clade depth for a trait in a phylogenetic

tree. NRI values indicate that cellulose responders clustered overall and at the tips of the phylogeny (NRI:  $4.49$ , NTI:  $1.43$ ) while xylose responders cluster terminally (NRI:  $-1.33$ , NTI:  $2.69$ ). The consenTRAIT clade depth for xylose and cellulose responders was  $0.012$  and  $0.028$  SSU rRNA gene sequence dissimilarity, respectively. As reference, the average clade depth is approximately  $0.017$  SSU rRNA gene sequence dissimilarity for arabinose (another five C sugar found in hemicellulose) utilization as inferred from genomic analyses, and was  $0.013$  and  $0.034$  SSU rRNA gene sequence dissimilarity for glucosidase and cellulase genomic potential, respectively [64, 66]. These results indicate xylose responders form terminal clusters dispersed throughout the phylogeny while cellulose responders form deep clades of terminally clustered OTUs.

## 500 Discussion

We identified microorganisms participating in soil C cycling using a nucleic acid SIP approach. Specifically, we observed assimilation of  $^{13}\text{C}$  from either  $^{13}\text{C}$ -xylose or  $^{13}\text{C}$ -cellulose into DNA for  $104$  OTUs from agricultural soil samples. We found  $^{13}\text{C}$  from  $^{13}\text{C}$ -xylose appeared to move into and then out of groups of related OTUs over time. By coupling nucleic acid SIP to high throughput sequencing we could diagnose OTU activity even when OTUs were at low relative abundance in non-fractionated DNA (e.g. on three occasions we did not detect responders in non-fractionated DNA). Our results support the degradative succession hypothesis, elucidate ecophysiological properties of soil microorganisms, reveal activity of widespread uncultured soil bacteria, and begin to piece together the microbial food web in soils.

The degradative succession hypothesis predicts an ecological transition in activity during the decomposition of plant matter from microbes that decompose labile plant biomass C to those that decompose structural more recalcitrant C. Our results concur with the degradative succession hypothesis. Microorganisms consumed xylose-C before cellulose-C and assimilated xylose-C into DNA faster than to cellulose-C. Xylose is major constituent of hemicellulose and is a labile component of fresh plant biomass. The phylogenetic composition of xylose responders changed between days 1, 3 and 7 and few OTUs appeared  $^{13}\text{C}$ -labeled in the  $^{13}\text{C}$ -xylose treatment after day 7. In the  $^{13}\text{C}$ -cellulose treatment few OTUs were  $^{13}\text{C}$ -labeled in the beginning of the experiment but  $^{13}\text{C}$  labelled OTUs increased at day 14 and maintained  $^{13}\text{C}$ -labelling through day 30. Finally, few (8 of 104) OTUs appeared to metabolize both xylose and cellulose demonstrating a succession in

activity from xylose responders to cellulose responders. In addition to agreeing with the degradative succession hypothesis, our results suggest complex interactions between microbes occur during labile C decomposition.

Correlations between community composition and environmental characteristics often indirectly reveal microorganisms that belong to ecologically consistent groups [67]. In this experiment, we directly identified ecological groups as a function of *in situ* metabolism and inferred group ecological strategies through phylogenetic affiliation. Several lines of evidence suggest xylose responders are able to grow rapidly and assimilate C from multiple sources. Xylose responders assimilated xylose-C into DNA within 24 hours and had low  $\Delta\hat{BD}$  relative to cellulose responders suggesting xylose was not the sole C source used for growth. Xylose represented 20% of the amendment and 3.5% of total soil C. Xylose responders often included the most abundant OTUs within the non-fractionated DNA and had high estimated *rrn* copy number relative to cellulose responders. However, to some degree, high *rrn* gene copy number may inflate observed xylose responder relative abundance. Notably, the majority of xylose responder SSU rRNA genes (86%) matched SSU rRNA genes from cultured isolates at high sequence identity (> 97%).

Cellulose responders, on the other hand, incorporated  $^{13}\text{C}$  into DNA after xylose responders and appeared to specialize in using cellulose as a C source. Cellulose responders grew over a span of weeks and had high  $\Delta\hat{BD}$  indicating cellulose remained the dominant C source for cellulose responders even though multiple sources of C were present (cellulose represented 6% of total C present in soil at the start of the experiment). Cellulose responders were also lower in relative abundance on average within the non-fractionated DNA and had lower estimated *rrn* copy number than xylose responders. The majority of cellulose responders were not close relatives of cultured isolates although a number of cellulose responders shared high SSU rRNA gene sequence identity with cultured *Proteobacteria* (e.g. *Cellvibrio*). We identified cellulose responders among phyla such as *Verrucomicrobia*, *Chloroflexi*, and *Planctomycetes* – phyla whose functions within soil communities remain unknown.

*Verrucomicrobia* made up 16% of the cellulose responders. *Verrucomicrobia* are cosmopolitan soil microbes [68] that can make up to 23% of SSU rRNA gene sequences in soils [68] and 9.8% of soil SSU rRNA [69]. Genomic analyses and laboratory experiments show that various isolates within the *Verrucomicrobia* are capable of

methanotrophy, diazotrophy, and cellulose degradation [70, 71]. Moreover, *Verrucomicrobia* have been hypothesized to degrade polysaccharides in many environments [72–74]. However, only one of the 15 most abundant verrucomicrobial phylotypes in global soil samples shared > 93% SSU rRNA gene sequence identity with a cultured isolate [68] and hence the role of soil *Verrucomicrobia* in global C-cycling remains unknown. The majority of verrucomicrobial cellulose responders belonged to two clades that fall within the *Spartobacteria*. *Spartobacteria* outnumbered all other *Verrucomicrobia* phylotypes in SSU rRNA gene surveys of 181 globally distributed soil samples [68]. Given their ubiquity and abundance in soil as well as their demonstrated incorporation of  $^{13}\text{C}$  from  $^{13}\text{C}$ -cellulose, *Verrucomicrobia* lineages, particularly *Spartobacteria*, may be important contributors to cellulose decomposition on a global scale.

Other notable cellulose responders include OTUs in the *Planctomycetes* and *Chloroflexi* both of which have previously been shown to assimilate  $^{13}\text{C}$  from  $^{13}\text{C}$ -cellulose added to soil [75]. *Planctomycetes* are common in soil [40], comprising 4 - 7% of bacterial cells in many soils [76, 77] and 7% +/- 5% of SSU rRNA [78]. Although soil *Planctomycetes* are widespread, their activities in soil remain poorly characterized. *Planctomycetes* represented 16% of cellulose responders and shared < 92% SSU rRNA gene sequence identity to their most closely related cultured isolates. *Chloroflexi* are known for metabolically dynamic lifestyles ranging from anoxygenic phototrophy to organohalide respiration [79] and are among the six most abundant bacterial phyla in soil [40]. Recent studies have focused on *Chloroflexi* roles in C cycling [79–81] and several *Chloroflexi* isolates use cellulose [79–81]. Four of the five *Chloroflexi* cellulose responders belong to a single clade within the *Herpetosiphonales*.

Finally, a single cellulose responder belonged to the *Melainabacteria* phylum (95% shared SSU rRNA gene sequence identity with *Vampirovibrio chlorellavorus*). The phylogenetic position of *Melainabacteria* is debated but *Melainabacteria* have been proposed to be a non-phototrophic sister phylum to *Cyanobacteria*. An analysis of a “*Melainabacteria*” genome [82] suggests the genomic capacity to degrade polysaccharides though *Vampirovibrio chlorellavorus* is an obligate predator of green alga [83]. The *Melainabacteria* cellulose responder did not respond to xylose so if it is predatory, it may prey specifically on structural C degraders.

Responders did not necessarily assimilate  $^{13}\text{C}$  into DNA directly from  $^{13}\text{C}$ -xylose or  $^{13}\text{C}$ -cellulose. In many ways, knowledge of secondary C degradation and/or microbial biomass turnover

may be more interesting with respect to the soil C-cycle than knowledge of primary degradation. The response to xylose suggests xylose-C moved through different trophic levels within the soil food web. The *Bacilli* degraded xylose first (65% of the xylose-C had been respired by day 1) representing 84% of day 1 xylose responders. *Bacilli* also comprised about 6% of SSU rRNA genes present in non-fractionated DNA on day 1. However, few *Bacilli* remained  $^{13}\text{C}$ -labeled by day 3 and their abundance declined reaching about 2% of soil SSU rRNA genes by day 30. Members of the *Bacillus* [84] and *Paenibacillus* in particular [59] have been previously implicated as labile C decomposers. The decline in relative abundance of *Bacilli* could be attributed to mortality and/or sporulation coupled to mother cell lysis. Concomitant with the decline in relative abundance and loss of  $^{13}\text{C}$ -label of *Bacilli*, *Bacteroidetes* OTUs appeared  $^{13}\text{C}$ -labeled at day 3. Finally, *Actinobacteria* appeared  $^{13}\text{C}$ -labeled at day 7 as *Bacteroidetes* xylose responders declined in relative abundance and became unlabeled. Hence, it seems reasonable to propose that *Bacteroidetes* and *Actinobacteria* OTUs became  $^{13}\text{C}$ -labeled via the consumption of  $^{13}\text{C}$ -labeled microbial biomass.

The inferred physiology of *Actinobacteria* and *Bacteroidetes* xylose responders provides further evidence that the activity dynamics represent C transfer between microbes by saprotrophy and/or predation. Most of the *Actinobacteria* xylose responders that appeared  $^{13}\text{C}$ -labeled at day 7 were members of the *Micrococcales* (Figure 3) and the most abundant  $^{13}\text{C}$ -labeled *Micrococcales* OTU at day 7 (OTU.4, Table S2) is annotated as belonging in the *Agromyces*. *Agromyces* are facultative predators that feed on the gram-positive *Luteobacter* in culture [85]. Additionally, certain types of *Bacteroidetes* can assimilate  $^{13}\text{C}$  from  $^{13}\text{C}$ -labeled *Escherichia coli* added to soil [86]. However, it is also possible that *Bacilli*, *Bacteroidetes*, and *Actinobacteria* are adapted to use xylose at different concentrations and that the observed activity dynamics resulted from changes in xylose concentration over time. If trophic transfer caused the activity dynamics, at least three different ecological groups exchanged carbon in 7 days. Models of the soil C cycle often exclude trophic interactions between soil bacteria (e.g. [87]), yet when soil C models do account for predators/saprophytes, trophic interactions are predicted to have significant effects on the fate of soil C [88].

**Implications for soil C cycling models.** Functional niche characterization for soil microorganisms is necessary to predict whether and how biogeochemical processes vary with microbial community composition. Functional niches are defined by soil

microbiologists have been incorporated into biogeochemical process models (E.g. [88, 89]). In some C models ecological strategies such as growth rate and substrate specificity are parameters for functional niche behavior [88]. The phylogenetic breadth of an functionally defined group is often inferred from the distribution of diagnostic genes across genomes [66] or from the physiology of isolates cultured on laboratory media [64]. For instance, the wide distribution of the glycolysis operon in microbial genomes is interpreted as evidence that many soil microorganisms participate in glucose turnover [10]. However, the functional niche may depend less on the distribution of diagnostic genes across genomes and more on life history traits that allow organisms to compete for a given substrate as it occurs in the soil. For instance, fast growth and rapid resuscitation allow microorganisms to compete for labile C which may often be transient in soil. Hence, life history traits may constrain the diversity of microbes that metabolize a given C source in the soil under a given set of conditions.

Biogeochemical processes mediated by a broad array of taxa are assumed to be less influenced by community change than narrow processes that involve a single, specific chemical transformation by a narrow suite of microbial participants [10, 90]. In addition, the diversity of a functionally defined group engaged in a specific C transformation is expected to correlate with C lability [10]. However, the diversity of active labile C and recalcitrant C decomposers in soil has not been directly quantified. We found comparable numbers of OTUs responded to  $^{13}\text{C}$ -cellulose and  $^{13}\text{C}$ -xylose (63 and 49, respectively). We also found that cellulose responders are phylogenetically clustered, and this suggests that the ability to degrade cellulose is phylogenetically conserved. The clade depth of cellulose responders, 0.028 SSU rRNA gene sequence dissimilarity, is on the same order as that observed for glycoside hydrolases which are diagnostic enzymes for cellulose degradation [66]. Xylose responders clustered in terminal branches indicating groups of closely related taxa used xylose but xylose responders also clustered phylogenetically with respect to time of first response (Figure 3, Figure 4). For example, xylose responders on day 1 are dominated by members of *Paenibacillus*. Thus, microorganisms that degraded labile C and structural C were both limited in diversity. Although the genes for xylose metabolism are likely widespread in the soil community it's possible limited groups of organisms had the ecological characteristics required to degrade xylose in soil under the conditions of this experiment. Therefore it's possible few phylogenetically coherent taxa actually participate in the metabolism

of labile C-sources under a given set of conditions, and hence changes in community composition may alter the dynamics of structural and labile C-transformations in soil.

Broadly, we observed labile C use by fast growing generalists and structural C use by slow growing specialists. These results agree with the MIM-ICS model which simulates leaf litter decomposition modeling the microbial community as two functionally defined groups, copiotrophs or oligotrophs [89]. Including these functional types improved the predictions of C storage in response to environmental change relative to models that did not consider any microbial physiological diversity. We identified microbial lineages engaged in labile and structural C decomposition or similarly speaking, copiotrophs and oligotrophs. We also observed potentially greater turnover – and at the very least rate differences in turnover – for copiotroph biomass relative to oligotroph biomass which may be important to consider when modeling microbial turnover input to SOM. It's also clear that there may be more than two vital functional types mediating C-cycling in soil. C in soil may travel through many microbial trophic levels where each C transfer represents an opportunity for C stabilization in association with soil minerals or C loss by respiration.

**Conclusion.** Microorganisms sequester atmospheric C and respire SOM influencing climate change on a global scale but we do not know which microorganisms carry out specific soil C transformations. In this experiment microbes from physiologically uncharacterized but cosmopolitan soil lineages participated in cellulose decomposition. Cellulose responders included members of the *Verrucomicrobia* (*Spartobacteria*), *Chloroflexi*, *Bacteroidetes* and *Planctomycetes*. *Spartobacteria* in particular are globally cosmopolitan soil microorganisms and are often the most abundant *Verrucomicrobia* order in soil [68]. Fast-growing aerobic spore formers from Firmicutes assimilated labile C in the form of xylose. Xylose responders within the *Bacteroidetes* and *Actinobacteria* are likely to have assimilated xylose C as a result of dynamic trophic exchange, mediated either by saprotrophy or predation. Our results suggest that, cosmopolitan *Spartobacteria* may degrade cellulose on a global scale, bacterial trophic interactions can significantly impact soil C cycling, and ecological traits are likely to act as a filter that constrains the diversity of microorganisms that are active *in situ* relative to those that have the genomic capacity for a given process.

## Methods

Additional information on sample collection and analytical methods is provided in Supplemental Materials and Methods.

Twelve soil cores (5 cm diameter x 10 cm depth) were collected from six sampling locations within an organically managed agricultural field in Penn Yan, New York. Soils were sieved (2 mm), homogenized, distributed into flasks (10 g in each 250 ml flask, n = 36) and equilibrated for 2 weeks. Soils were amended with a mixture containing 5.3 mg C g<sup>-1</sup> soil dry weight (d.w.) and brought to 50% water holding capacity. The mixture contained 38% cellulose, 23% lignin, 20% xylose, 3% arabinose, 1% galactose, 1% glucose, and 0.5% mannose by mass, with the remaining 13.5% mass composed of an amino acid (in-house made replica of Teknova C0705) and macronutrient mixture (Murashige and Skoog, Sigma Aldrich M5524). This mixture approximates the molecular composition of switchgrass biomass with hemicellulose replaced by its constituent monomers [91]. Three parallel treatments were performed which varied the isotopic composition of the mixture: (1) unlabeled control, (2) <sup>13</sup>C-cellulose (synthesized as described in Supplemental Methods), (3) <sup>13</sup>C-xylose (98 atom% <sup>13</sup>C, Sigma Aldrich). A total of 12 microcosms were established per treatment. Other details relating to substrate addition can be found in Supplemental Methods. Microcosms were sampled destructively at days 1 (control and xylose only), 3, 7, 14, and 30 and soils were stored at -80°C until nucleic acid extraction. The abbreviation 13CXPS refers to the 13C-xylose treatment (<sup>13</sup>C Xylose Plant Simulant), 13CCPS refers to the <sup>13</sup>C treatment and 12CCPS refers to the unlabeled control.

Nucleic acids were extracted using a modified Griffiths protocol [92] and DNA was prepared for isopycnic centrifugation as previously described (Reference 55). A total of 5 g of DNA was added to each 4.7 ml CsCl density gradient composed of 1.69 g ml<sup>-1</sup> CsCl in 15 mM Tris-HCl, 15 mM EDTA, 15 mM KCl. Centrifugation was performed in a TLA-110 rotor at 55,000 rpm and 20C for 66 hr. Fractions of 100 L were collected by displacement at 3.3  $\mu$ L s<sup>-1</sup> [44] into Acroprep 96 filter plates (Pall Life Sciences 5035). The refractive index of each fraction was measured immediately using a Reichart AR200 digital refractometer as previously described [51]. The DNA was desalted by washing (3 x 200  $\mu$ L) with TE in the Acroprep filter wells followed by resuspension in 50  $\mu$ L TE. SSU rRNA genes were amplified from gradient fractions (n = 20 per gradient) and from non-fractionated DNA. Barcoded primers consisted of: 454-specific adapter B, a 10 bp barcode [93], a 2 bp linker (5-CA-3), and 806R primer for re-

verse primer (BA806R); and 454-specific adapter A, a 2 bp linker (5-TC-3), and 515F primer for forward primer (BA515F). Each PCR contained 1.25 U  $\mu\text{l}^{-1}$  AmpliTaq Gold (Life Technologies, Grand Island, NY; N8080243), 1X Buffer II (100 mM Tris-HCl, 500 mM KCl, pH 8.3), 2.5 mM MgCl<sub>2</sub>, 200  $\mu\text{M}$  of each dNTP, 0.5 mg ml<sup>-1</sup> BSA, 0.2  $\mu\text{M}$  BA515F, 0.2  $\mu\text{M}$  BA806R, and 10  $\mu\text{l}$  of 1:30 DNA template in 25  $\mu\text{l}$  total volume). Reactions were performed in triplicate and pooled. Amplified DNA was gel purified using the Wizard SV gel and PCR clean-up system (Promega, Madison, WI; A9281) per manufacturers protocol. Samples were normalized by SequalPrep normalization plates (Invitrogen, Carlsbad, CA; A10510) and pooled in equimolar concentration. Amplicons were sequenced on Roche 454 FLX system using titanium chemistry at Selah Genomics (Columbia, SC).

SSU rRNA gene sequences were initially screened by maximum expected errors at a specific read length threshold [94]. Reads that had more than 0.5 expected errors at a length of 250 nt were discarded. The remaining reads were aligned to the Silva Reference Alignment as provided in the Mothur software package using the Mothur NAST aligner [95, 96]. Reads that did not align to the expected region of the SSU rRNA gene were discarded. After expected error and alignment based quality control. The remaining quality controlled reads were annotated using the UClust taxonomic annotation framework in [97, 98]. We used 97% cluster seeds from the Silva SSU rRNA database (release 111Ref) [99] as reference for taxonomic annotation (provided on the QIIME website) [99]. Quality control screening filtered out 344,472 or 1,720,480 raw sequencing reads. Reads annotated as “Chloroplast”, “Eukaryota”, “Archaea”, “Unassigned” or “mitochondria” were culled from the dataset. Sequences were distributed into OTUs with a centroid based clustering algorithm (i.e. UPARSE [94]). The centroid selection also included robust chimera screening [94]. OTU centroids were established at a threshold of 97% sequence identity and non-centroid sequences were mapped back to centroids. Reads that could not be mapped to an OTU centroid at greater than or equal to 97% sequence identity were discarded. For phylogenetic reconstruction, alignment was performed with SSU-Align [100, 101]. Columns in the alignment that were aligned with poor confidence (< 95% of characters had posterior probability > 95%) were not considered when building the phylogenetic tree. Additionally, the alignment was trimmed to coordinates such that all sequences in the alignment began and ended at the same positions. FastTree [102] was used with default parameters to build the phylogeny. NMDS ordination

was performed on weighted Unifrac [103] distances between samples. The Phyloseq [104] wrapper for Vegan [105] (both R packages) was used to compute sample values along NMDS axes. The ‘adonis’ function in Vegan was used to perform Adonis tests (default parameters) [60].

We used DESeq2 (R package), an RNA-Seq differential expression statistical framework [106], to identify OTUs that were enriched in high density gradient fractions from <sup>13</sup>C-treatments relative to corresponding density fractions from control treatments (for review of RNA-Seq differential expression statistics applied to microbiome OTU count data see (30)). We define “high density gradient fractions” as gradient fractions whose density falls between 1.7125 and 1.755 g ml<sup>-1</sup>. Briefly, DESeq2 includes several features that enable robust estimates of standard error in addition to reliable ranking of logarithmic fold change (LFC) in abundance (i.e. gamma-Poisson regression coefficients) even with low count groups where LFC can often be noisy. Further, statistical evaluation of LFC can be performed with selected thresholds as opposed to the often default null hypothesis that differential abundance for an OTU is exactly zero. This enables the most biologically interesting OTUs to be selected for subsequent analyses. We calculated LFC and corresponding standard errors for comparisons between <sup>13</sup>C treatments and control (high density fractions only) for each OTU. Subsequently, a one-sided Wald test was used to statistically assess LFC values (using corresponding standard errors). The user-defined null hypothesis for the Wald test was that LFC was less than one standard deviation above the mean of all LFC values. P-values were corrected for multiple comparisons by using the Benjamini and Hochberg method [107]. Independent filtering was performed on the basis of sparsity prior to correcting P-values for multiple comparisons. The sparsity value that yielded the most P-values less than 0.10 was selected for independent filtering by sparsity. Briefly, OTUs were eliminated if they failed to appear in at least 45% of high density gradient fractions for a given <sup>13</sup>C/control treatment pair, these OTUs are unlikely to have sufficient data to allow for the determination of statistical significance.

## References

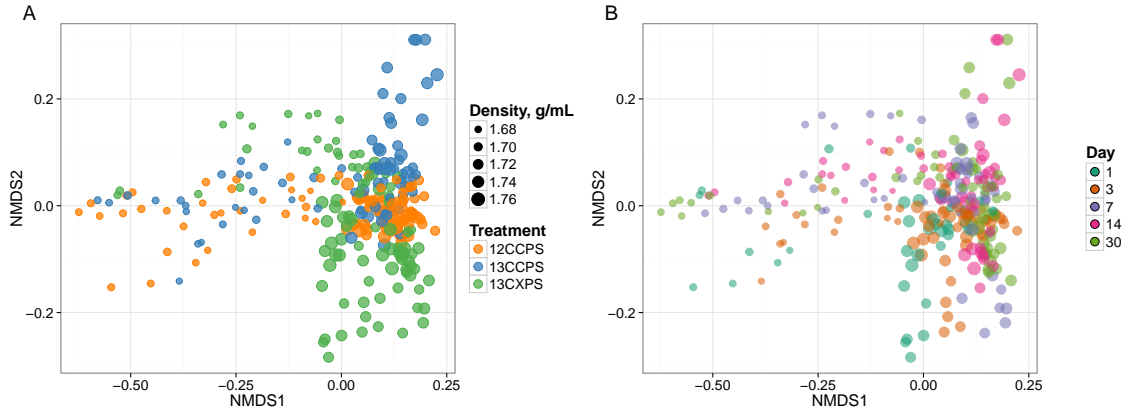
1. Amundson R (2001) The carbon budget in soils. *Annu Rev Earth Planet Sci* 29(1): 535–562.
2. Batjes N-H (1996) Total carbon and nitrogen in the soils of the world. *European Journal of Soil Science* 47(2): 151–163.
3. Chapin F (2002) Principles of terrestrial ecosystem ecology.

4. Allison S-D, Wallenstein M-D, Bradford M-A (2010) Soil-carbon response to warming dependent on microbial physiology. *Nature Geoscience* 3(5): 336–340. <sup>995</sup>
5. Six J, Frey S-D, Thiet R-K, Batten K-M (2006) Bacterial and Fungal Contributions to Carbon Sequestration in Agroecosystems. *Soil Science Society of America Journal* 70(2): 555. <sup>1000</sup>
6. Treseder K-K, Balser T-C, Bradford M-A, Brodie E-L, Dubinsky E-A, Evener V-T, et al. (2011) Integrating microbial ecology into ecosystem models: challenges and priorities. *Biogeochemistry* 109(1-3): 7–18. <sup>1005</sup>
7. Wieder W-R, Bonan G-B, Allison S-D (2013) Global soil carbon projections are improved by modelling microbial processes. *Nature Climate Change* 3(10): 909–912. <sup>1010</sup>
8. Bradford M-A, Fierer N, Reynolds J-F (2008) Soil carbon stocks in experimental mesocosms are dependent on the rate of labile carbon, nitrogen and phosphorus inputs to soils. *Functional Ecology* 22(6): 964–974. <sup>1015</sup>
9. Neff J-C, Asner G-P (2001) Dissolved organic carbon in terrestrial ecosystems: synthesis and a model. *Ecosystems* 4(1): 29–48.
10. McGuire K-L, Treseder K-K (2010) Microbial communities and their relevance for ecosystem models: Decomposition as a case study. *Soil Biology and Biochemistry* 42(4): 529–535. <sup>1020</sup>
11. Lynd L-R, Weimer P-J, van Zyl W-H, Pretorius I-S (2002) Microbial cellulose utilization: fundamentals and biotechnology. *Microbiology and molecular biology reviews: MMBR* 66(3): 506–table of contents. <sup>1025</sup>
12. Saha B-C (2003) Hemicellulose bioconversion. *Journal of Industrial Microbiology & Biotechnology* 30(5): 279–291. <sup>1030</sup>
13. Sun X-F, Xu F, Zhao H, Sun R-C, Fowler P, Baird M-S (2005) Physicochemical characterisation of residual hemicelluloses isolated with cyanamide-activated hydrogen peroxide from organosolv pre-treated wheat straw. *Bioresource Technology* 96(12): 1342–1349. <sup>1035</sup>
14. Bunnell K, Rich A, Luckett C, Wang Y-J, Martin E, Carrier D-J (2013) Plant Maturation Effects on the Physicochemical Properties and Dilute Acid Hydrolysis of Switchgrass (*Panicum virgatum*, L.) Hemicelluloses. *ACS Sustainable Chemistry & Engineering* 1(6): 649–654. <sup>1040</sup>
15. Garrett S-D (1951) Ecological Groups of Soil Fungi: A Survey of Substrate Relationships. *New Phytologist* 50(2): 149–166. <sup>1045</sup>
16. Alexander M (1964) Biochemical Ecology of Soil Microorganisms. *Annual Review of Microbiology* 18(1): 217–250. <sup>1050</sup>
17. Engelking B, Flessa H, Joergensen R-G (2007) Microbial use of maize cellulose and sugarcane sucrose monitored by changes in the 13C/12C ratio. *Soil Biology and Biochemistry* 39(8): 1888–1896.
18. Hu S, van Bruggen A-H-C (1997) Microbial Dynamics Associated with Multiphasic Decomposition of 14C-Labeled Cellulose in Soil. *Microbial Ecology* 33(2): 134–143.
19. Rui J, Peng J, Lu Y (2009) Succession of Bacterial Populations during Plant Residue Decomposition in Rice Field Soil. *Applied and Environmental Microbiology* 75(14): 4879–4886.
20. Bastian F, Bouziri L, Nicolardot B, Ranjard L (2009) Impact of wheat straw decomposition on successional patterns of soil microbial community structure. *Soil Biology and Biochemistry* 41(2): 262–275.
21. Garrett S-D (1963) Soil Fungi and Soil Fertility.
22. Bremer E, Kuikman P (1994) Microbial utilization of 14C[U]glucose in soil is affected by the amount and timing of glucose additions. *Soil Biology and Biochemistry* 26(4): 511–517.
23. Frankland J-C (1998) Fungal succession – unravelling the unpredictable. *Mycological Research* 102(1): 1–15.
24. Osono T (2005) Colonization and succession of fungi during decomposition of Swida controversa leaf litter. *Mycologia* 97(3): 589–597.
25. Coleman D-C, Crossley D-A (1996) Fundamentals of Soil Ecology.
26. Nannipieri P, Ascher J, Ceccherini M-T, Landi L, Pietramellara G, Renella G (2003) Microbial diversity and soil functions. *European Journal of Soil Science* 54(4): 655–670.
27. Strickland M-S, Lauber C, Fierer N, Bradford M-A (2009) Testing the functional significance of microbial community composition. *Ecology* 90(2): 441–451.
28. Zak D-R, Blackwood C-B, Waldrop M-P (2006) A molecular dawn for biogeochemistry. *Trends in Ecology & Evolution* 21(6): 288–295.
29. Reed H-E, Martiny J-BH (2007) Testing the functional significance of microbial composition in natural communities. *FEMS Microbiology Ecology* 62(2): 161–170.
30. Schimel J-P, Schaeffer S-M (2012) Microbial control over carbon cycling in soil. *Frontiers in Microbiology* 3: 348. doi: 10.3389/fmicb.2012.00348
31. Allison S-D, Martiny J-BH (2008) Resistance resilience, and redundancy in microbial communities. *Proc Natl Acad Sci USA* 105(Supplement 1): 11512–11519.

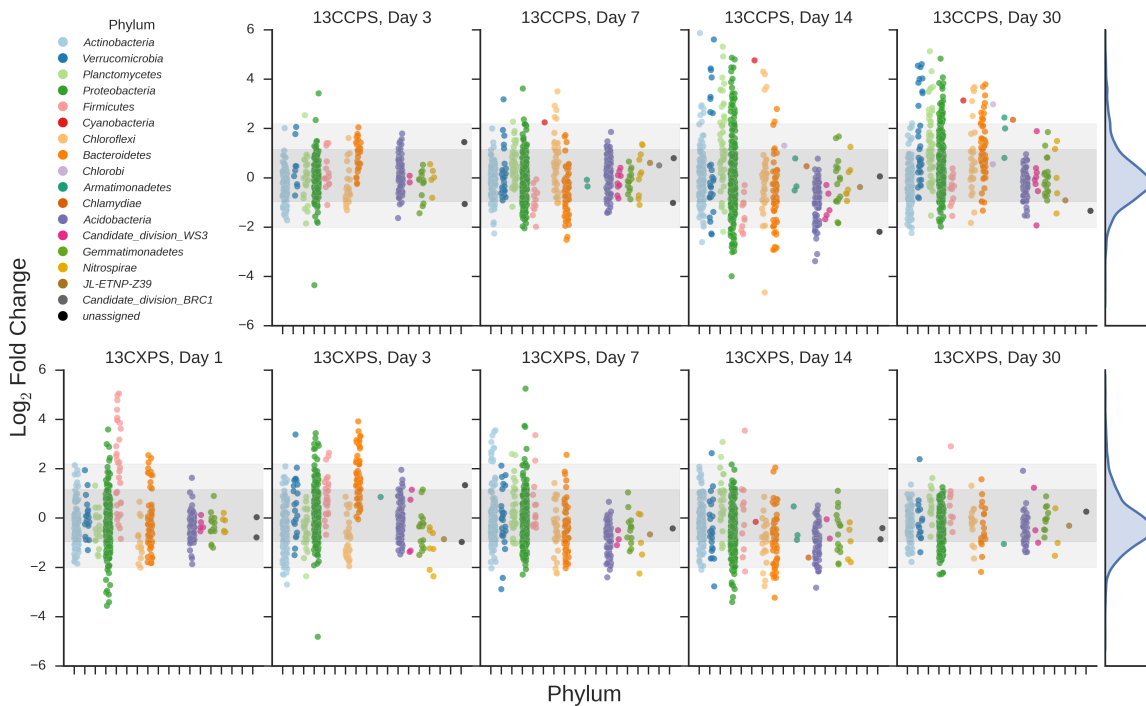
- 1110 34. Cavigelli M-A, Robertson G-P (2000) The functional significance of denitrifier community composition in a terrestrial ecosystem.<sup>1170</sup> *Ecology* 81(5): 1402–1414.
- 1115 35. Carney K-M, Matson P-A, Bohannan B-JM (2004) Diversity and composition of tropical soil nitrifiers across a plant diversity gradient and among land-use types. *Ecology Letters* 7(8): 684–694.
- 1120 36. Hawkes C-V, Wren I-F, Herman D-J, Firestone M-K (2005) Plant invasion alters nitrogen cycling by modifying the soil nitrifying community. *Ecology Letters* 8(9): 976–985. <sup>1180</sup>
- 1125 37. Webster G, Embley T-M, Freitag T-E, Smith Z, Prosser J-I (2005) Links between ammonia oxidizer species composition, functional diversity and nitrification kinetics in grassland soils. *Environmental Microbiology* 7(5):<sup>1185</sup> 676–684.
- 1130 38. Gulledge J, Doyle A-P, Schimel J-P (1997) Different NH<sub>4</sub><sup>+</sup>-inhibition patterns of soil CH<sub>4</sub> consumption: A result of distinct CH<sub>4</sub>-oxidizer populations across sites? *Soil Biology and Biochemistry* 29(1): 13–21.
- 1135 39. Hsu S-F, Buckley D-H (2009) Evidence for the functional significance of diazotroph community structure in soil. *The ISME journal* 3(1): 124–136. <sup>1195</sup>
- 1140 40. Janssen P-H (2006) Identifying the dominant soil bacterial taxa in libraries of 16S rRNA and 16S rRNA genes. *Appl Environ Microbiol* 72(3): 1719–1728.
- 1145 42. Chen Y, Murrell J-C (2010) When metagenomics meets stable-isotope probing: progress and perspectives. *Trends Microbiol* 18(4): 157–163.
- 1150 43. Radajewski S, Ineson P, Parekh N-R, Murrell J-C (2000) Stable-isotope probing as<sup>1205</sup> tool in microbial ecology. *Nature* 403(6770): 646–649.
- 1155 44. Manefield M, Whiteley A-S, Griffiths R-I, Bailey M-J (2002) RNA Stable isotope probing: a novel means of linking microbial community function to phylogeny. *Appl Environ Microbiol* 68(11): 5367–5373.
- 1160 45. McDonald I-R, Radajewski S, Murrell J-C (2005) Stable isotope probing of nucleic acids in methanotrophs and methylotrophs: A re-<sup>1215</sup>view. *Org Geochim* 36(5): 779–787.
- 1165 46. Morris S-A, Radajewski S, Willison T-W, Murrell J-C (2002) Identification of the functionally active methanotroph population in a peat soil microcosm by stable-isotope probing. *Appl Environ Microbiol* 68(3): 1446–1453.
- 1170 47. Hutchens E, Radajewski S, Dumont M-G, McDonald I-R, Murrell J-C (2004) Analysis of methanotrophic bacteria in Movile Cave by<sup>1220</sup>
- stable isotope probing. *Environmental Microbiology* 6(2): 111–120.
48. Lueders T, Manefield M, Friedrich M (2004) Enhanced sensitivity of DNA- and rRNA-based stable isotope probing by fractionation and quantitative analysis of isopycnic centrifugation gradients.. ???: 6: 73–8.
49. DeRito C-M, Pumphrey G-M, Madsen E-L (2005) Use of field-based stable isotope probing to identify adapted populations and track carbon flow through a phenol-degrading soil microbial community. *Applied and Environmental Microbiology* 71(12): 7858–7865.
50. Ziegler S-E, White P-M, Wolf D-C, Thoma G-J (2005) Tracking the fate and recycling of <sup>13</sup>C-labeled glucose in soil. *Soil Sci* 170(10): 767–778.
51. Buckley D-H, Huangyutitham V, Hsu S-F, Nelson T-A (2007) Stable isotope probing with <sup>15</sup>N achieved by disentangling the effects of genome G+C content and isotope enrichment on DNA density. *Appl Environ Microbiol* 73(10): 3189–3195.
52. Birnir G-D (1978) Centrifugal separations: Molecular and cell biology.
53. Holben W-E, Harris D (1995) DNA-based monitoring of total bacterial community structure in environmental samples. *Molecular Ecology* 4(5): 627–632.
54. Nisslein K, Tiedje J-M (1999) Soil Bacterial Community Shift Correlated with Change from Forest to Pasture Vegetation in a Tropical Soil. *Applied and Environmental Microbiology* 65(8): 3622–3626.
55. Lu Y, Conrad R (2005) In situ stable isotope probing of methanogenic archaea in the rice rhizosphere. *Science* 309(5737): 1088–1090.
56. Lueders T, Pommerenke B, Friedrich M-W (2004) Stable-isotope probing of microorganisms thriving at thermodynamic limits: syntrophic propionate oxidation in flooded soil. *Appl. Environ. Microbiol.* 70(10): 5778–5786.
57. DeRito C-M, Pumphrey G-M, Madsen E-L (2005) Use of field-based stable isotope probing to identify adapted populations and track carbon flow through a phenol-degrading soil microbial community. *Appl. Environ. Microbiol.* 71(12): 7858–7865.
58. Aoyagi T, Hanada S, Itoh H, Sato Y, Ogata A, Friedrich M-W, et al. (2015) Ultra-high-sensitivity stable-isotope probing of rRNA by high-throughput sequencing of isopycnic centrifugation gradients. *Environmental Microbiology Reports* 7(2): 282–287.
59. Verastegui Y, Cheng J, Engel K, Kolczynski D, Mortimer S, Lavigne J, et al. (2014) Multisubstrate isotope labeling and metagenomic analysis of active soil bacterial communities.

- mBio* 5(4): e01157–14.
60. Anderson M-J (2001) A new method for non-parametric multivariate analysis of variance. *Austral Ecology* 26(1): 32–46.
  61. Kembel S-W, Wu M, Eisen J-A, Green J-L (2012) Incorporating 16S gene copy number information improves estimates of microbial diversity and abundance. *PLoS Comput Biol* 8(10): e1002743.
  62. Klappenbach J-A, Dunbar J-M, Schmidt T-M (2000) rRNA Operon copy number reflects ecological strategies of bacteria. *Appl Environ Microbiol* 66(4): 1328–1333.
  63. Webb C-O (2000) Exploring the phylogenetic structure of ecological communities: an example for rain forest trees.. *The American Naturalist* 156(2): 145–155.
  64. Martiny A-C, Treseder K, Pusch G (2013) Phylogenetic conservatism of functional traits in microorganisms. *ISMEJ* 7(4): 830–838.
  65. Evans S-E, Wallenstein M-D (2014) Climate change alters ecological strategies of soil bacteria. *Ecol Lett* 17(2): 155–164.
  66. Berlemon R, Martiny A-C (2013) Phylogenetic distribution of potential cellulases in bacteria. *Appl Environ Microbiol* 79(5): 1545–1554.
  67. Fierer N, Bradford M-A, Jackson R-B (2007) Toward an ecological classification of soil bacteria. *Ecology* 88(6): 1354–1364.
  68. Bergmann G-T, Bates S-T, Eilers K-G, Lauber C-L, Caporaso J-G, Walters W-A, et al. (2011) The under-recognized dominance of Verrucomicrobia in soil bacterial communities. *Soil Biology and Biochemistry* 43(7): 1450–1455.
  69. Buckley D-H, Schmidt T-M (2001) Environmental factors influencing the distribution of rRNA from Verrucomicrobia in soil. *FEMS Microbiol Ecol* 35(1): 105–112.
  70. Wertz J-T, Kim E, Breznak J-A, Schmidt T-M, Rodrigues J-LM (2011) Genomic and physiological characterization of the verrucomicrobia isolate *diplosphaera colitermitum* gen. nov. sp. nov., reveals microaerophily and nitrogen fixation genes. *Appl Environ Microbiol* 78(5): 1544–1555.
  71. Otsuka S, Ueda H, Suenaga T, Uchino Y, Hamada M, Yokota A, et al. (2012) Roseimicrobium gellanolyticum gen. nov. sp. nov., a new member of the class Verrucomicrobiae. *Int J Syst Evol Microbiol* 63(Pt 6): 1982–1986.
  72. Fierer N, Ladau J, Clemente J-C, Leff J-W, Owens S-M, Pollard K-S, et al. (2013) Reconstructing the microbial diversity and function of pre-agricultural tallgrass prairie soils in the united states. *Science* 342(6158): 621–624.
  73. Chin K-J, Hahn D, Hengstmann U, Liesack W, Janssen P-H (1999) Characterization and identification of numerically abundant culturable bacteria from the anoxic bulk soil of rice paddy microcosms. *Appl Environ Microbiol* 65(11): 5042–5049.
  74. Herlemann D-PR, Lundin D, Labrenz M, Jürgens K, Zheng Z, Aspeborg H, et al. (2013) Metagenomic de novo assembly of an aquatic representative of the verrucomicrobial class spartobacteria. *mBio* 4(3): e0056912.
  75. Schellenberger S, Kolb S, Drake H-L (2010) Metabolic responses of novel cellulolytic and saccharolytic agricultural soil Bacteria to oxygen. *Environ Microbiol* 12(4): 845–861.
  76. Zarda B, Hahn D, Chatzinotas A, Schnhuber W, Neef A, Amann R-I, et al. (1997) Analysis of bacterial community structure in bulk soil by in situ hybridization. *Archives of Microbiology* 168(3): 185–192.
  77. Chatzinotas A, Sandaa R-A, Schnhuber W, Amann R, Daee F-L, Torsvik V, et al. (1998) Analysis of broad-scale differences in microbial community composition of two pristine forest soils. *Syst Appl Microbiol*. 21(4): 579–587.
  78. Buckley D-H, Schmidt T-M (2003) Diversity and dynamics of microbial communities in soils from agro-ecosystems. *Environ. Microbiol.* 5(6): 441–452.
  79. Hug L-A, Castelle C-J, Wrighton K-C, Thomas B-C, Sharon I, Frischkorn K-R, et al. (2013) Community genomic analyses constrain the distribution of metabolic traits across the Chloroflexi phylum and indicate roles in sediment carbon cycling. *Microbiome* 1(1): 22.
  80. Goldfarb K-C, Karaoz U, Hanson C-A, Santee C-A, Bradford M-A, Treseder K-K, et al. (2011) Differential Growth Responses of Soil Bacterial Taxa to Carbon Substrates of Varying Chemical Recalcitrance. *Frontiers in Microbiology* 2: 94. doi: 10.3389/fmicb.2011.00094
  81. Cole J-K, Gieler B-A, Heisler D-L, Palisoc M-M, Williams A-J, Dohnalkova A-C, et al. (2013) Kallotenu papyrolyticum gen. nov. sp. nov., a cellulolytic and filamentous thermophile that represents a novel lineage (Kallotenuales ord. nov., Kallotenuaceae fam. nov.) within the class Chloroflexia. *Int J Syst Evol Microbiol* 63(Pt 12): 4675–4682.
  82. Rienzi S-CD, Sharon I, Wrighton K-C, Koren O, Hug L-A, Thomas B-C, et al. (2013) The human gut and groundwater harbor non-photosynthetic bacteria belonging to a new candidate phylum sibling to Cyanobacteria. *eLIFE* 2: e01102.

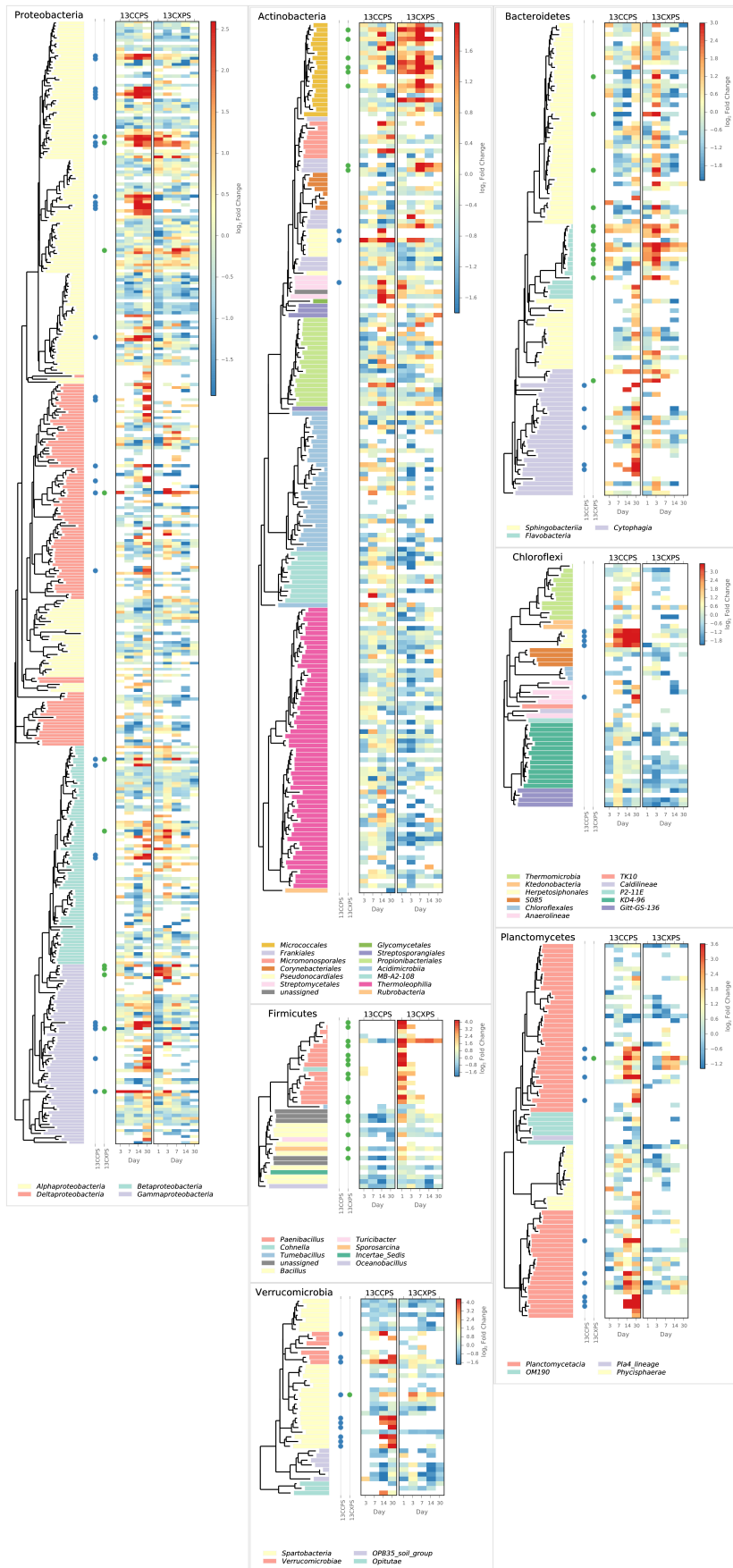
83. Gromov B-V, Mamkaeva K-A (1972) [Electron microscopic study of parasitism by Bdellovibrio chlorellavorus bacteria on cells of the green alga Chlorella vulgaris]. *Tsitolgiia* 14(2): 256–260.
- 1345 84. Cleveland C-C, Nemergut D-R, Schmidt S-K, Townsend A-R (2007) Increases in soil respiration following labile carbon additions linked to rapid shifts in soil microbial community composition. ??? 82(3): 229–240.
- 1350 85. Casida L-E (1983) Interaction of *Agromyces ramosus* with other bacteria in soil. *Appl Environ Microbiol* 46(4): 881–888.
- 1355 86. Lueders T, Kindler R, Miltner A, Friedrich M-W, Kaestner M (2006) Identification of bacterial micropredators distinctively active in a soil microbial food web. *Appl Environ Microbiol* 72(8): 5342–5348.
- 1360 87. Moore J-C, Walter D-E, Hunt H-W (1988) Arthropod Regulation of Micro- and Mesobiota in Below-Ground Detrital Food Webs. *Annu Rev Entomol* 33(1): 419–435.
- 1365 88. Kaiser C, Franklin O, Dieckmann U, Richter A (2014) Microbial community dynamics alleviate stoichiometric constraints during litter decay. *Ecol Lett* 17(6): 680–690.
- 1370 89. Wieder W-R, Grandy A-S, Kallenbach C-M, Bonan G-B (2014) Integrating microbial physiology and physio-chemical principles in soils with the MIcrobial-MIneral Carbon Stabilization (MIMICS) model. *Biogeosciences* 11(14): 3899–3917.
- 1375 90. Schimel J (1995) Ecosystem consequences of microbial diversity and community structure. *Arctic and alpine biodiversity: patterns, causes and ecosystem consequences*, , eds. III P-DFSC, Körner P-DC, Ecological Studies (Springer, Berlin Heidelberg), pp 239–254.
- 1380 91. Schnellenberger K, Demin D, Stahr K, Kuzyakov Y (2008) Microbial utilization and mineralization of  $^{14}\text{C}$  glucose added in six orders of concentration to soil. *Soil Biology and Biochemistry* 40(8): 1981–1988.
- 1385 92. Griffiths R-I, Whiteley A-S, O'Donnell A-G, Bailey M-J (2000) Rapid method for coextraction of DNA and RNA from natural environments for analysis of ribosomal DNA- and rRNA-based microbial community composition. *Appl Environ Microbiol* 66(12): 5488–5491.
- 1390 93. Hamady M, Walker J-J, Harris J-K, Gold N-J, Knight R (2008) Error-correcting barcoded primers for pyrosequencing hundreds of samples in multiplex. *Nat Meth* 5(3): 235–237.
- 1395 94. Edgar R-C (2013) UPARSE: highly accurate OTU sequences from microbial amplicon reads. *Nat. Methods* 10(10): 996–998.
95. DeSantis T-Z, Hugenholtz P, Keller K, Brodie E-L, Larsen N, Piceno Y-M, et al. (2006) NAST: a multiple sequence alignment server for comparative analysis of 16S rRNA genes. *Nucleic Acids Research* 34(suppl 2): W394–W399.
96. Schloss P-D, Westcott S-L, Ryabin T, Hall J-R, Hartmann M, Hollister E-B, et al. (2009) Introducing mothur: open-source, platform-independent, community-supported software for describing and comparing microbial communities. *Appl. Environ. Microbiol.* 75(23): 7537–7541.
97. ??? (2010) QIIME allows analysis of high-throughput community sequencing data. *Nat. Methods* 7(5): 335–336.
98. Edgar R-C (2010) Search and clustering orders of magnitude faster than BLAST. *Bioinformatics* 26(19): 2460–2461.
99. Quast C, Pruesse E, Yilmaz P, Gerken J, Schweer T, Yarza P, et al. (2013) The SILVA ribosomal RNA gene database project: improved data processing and web-based tools. *Nucleic Acids Res.* 41: D590–596.
100. Nawrocki E-P, Kolbe D-L, Eddy S-R (???) Infernal 1.0: inference of RNA alignments. *Bioinformatics* 25(10): 1335–1337.
101. Nawrocki E-P, Eddy S-R (2013) Infernal 1.1: 100-fold faster RNA homology searches. *Bioinformatics* 29(22): 2933–2935.
102. Price M-N, Dehal P-S, Arkin A-P (2010) FastTree2 - approximately maximum-likelihood trees for large alignments. *PLoS ONE* 5(3): e9490.
103. Lozupone C, Knight R (???) UniFrac: a new phylogenetic method for comparing microbial communities. *Appl. Environ. Microbiol.* 71(12): 8228–8235.
104. McMurdie P-J, Holmes S (2013) phyloseq: an R package for reproducible interactive analysis and graphics of microbiome census data. *PLoS ONE* 8(4): e61217.
105. Oksanen J, Blanchet F-G, Kindt R, Legendre P, Minchin P-R, O'Hara R-B, et al. (2015) vegan: Community Ecology Package.
106. Love M-I, Huber W, Anders S (2014) Moderated estimation of fold change and dispersion for RNA-seq data with DESeq2. *Genome Biol.* 15(12): 550.
107. Benjamini Y, Hochberg Y (???) Controlling the false discovery rate: A practical and powerful approach to multiple testing. *Journal of the Royal Statistical Society. Series B (Methodological)* 57(1): 289–300.



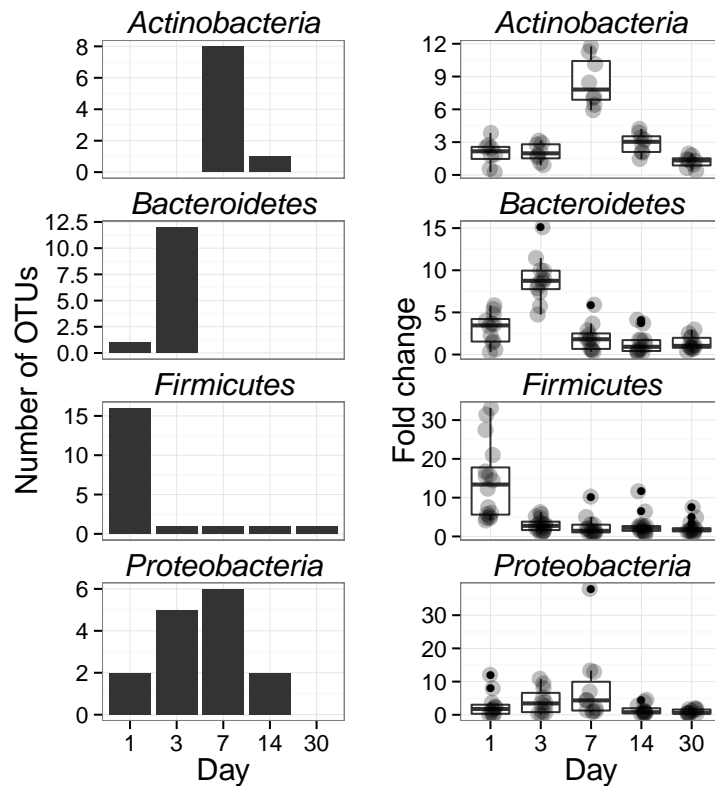
**Fig. 1.** NMDS analysis from weighted unifrac distances of 454 sequence data from SIP fractions of each treatment over time. Twenty fractions from a CsCl gradient fractionation for each treatment at each time point were sequenced (Fig. S1). Each point on the NMDS represents the bacterial composition based on 16S sequencing for a single fraction where the size of the point is representative of the density of that fraction and the colors represent the treatments (A) or days (B).



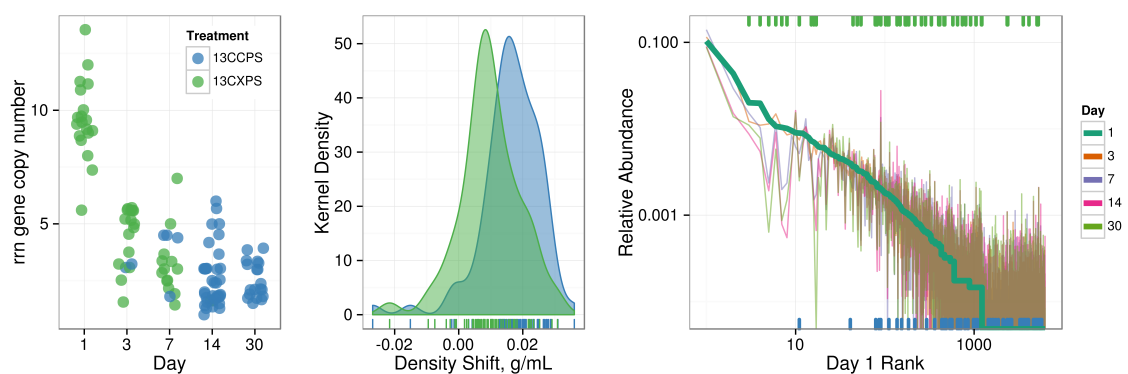
**Fig. 2.** Log<sub>2</sub> fold change of <sup>13</sup>C-responders in cellulose treatment (top) and xylose treatment (bottom). Log<sub>2</sub> fold change is based on the relative abundance in the experimental treatment compared to the control within the density range 1.7125–1.755 g ml<sup>-1</sup>. Taxa are colored by phylum. The last column shows the distribution of all fold change values in each row. The darker gray band represents one standard deviation and the lighter band represents two standard deviations about the mean of all fold change values for both treatments.



**Fig. 3.** Phylum specific trees. Heatmap indicates fold change between heavy fractions of control gradients versus labeled gradients. Dots indicate the position of "responders" to  $^{13}\text{C}$ -xylose (green) or  $^{13}\text{C}$ -cellulose (blue).

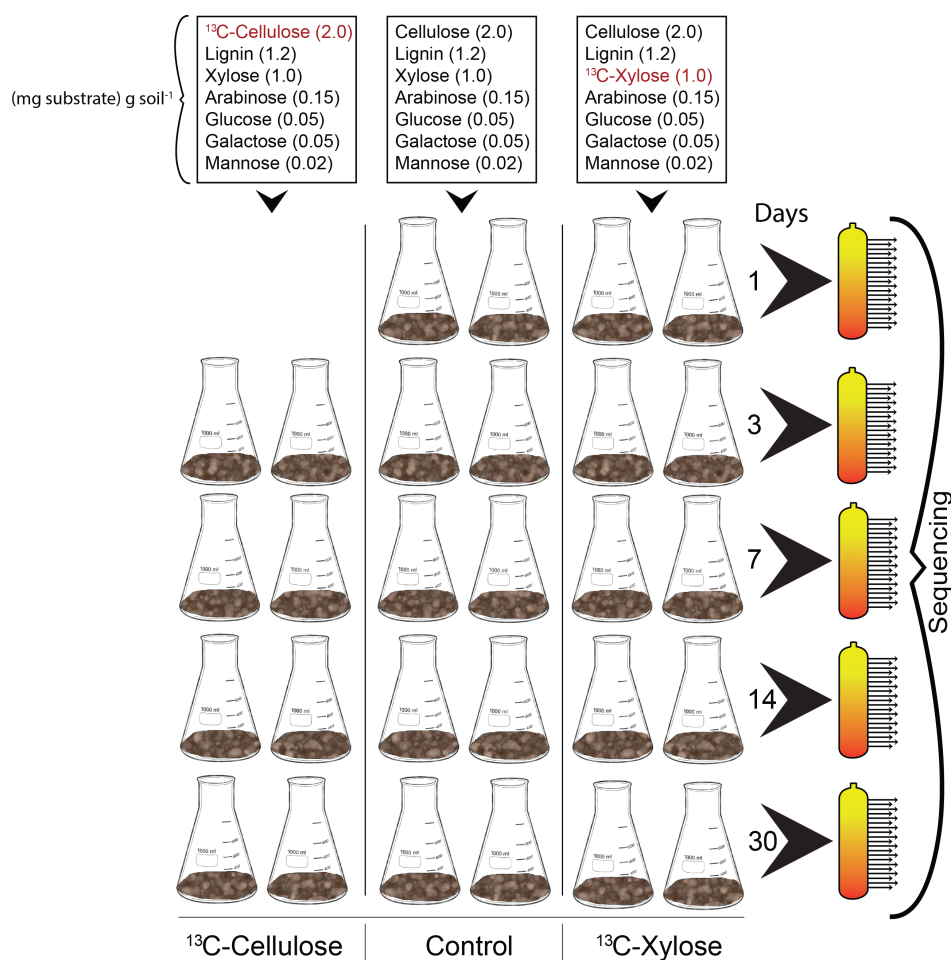


**Fig. 4.** Left column shows counts of  $^{13}\text{C}$ -xylose responders in the *Actinobacteria*, *Bacteroidetes*, *Firmicutes* and *Proteobacteria* at days 1, 3, 7 and 30. Right panel shows OTU fold enrichment in heavy gradient fractions for  $^{13}\text{C}$ -xylose amendment DNA relative to corresponding control fractions.

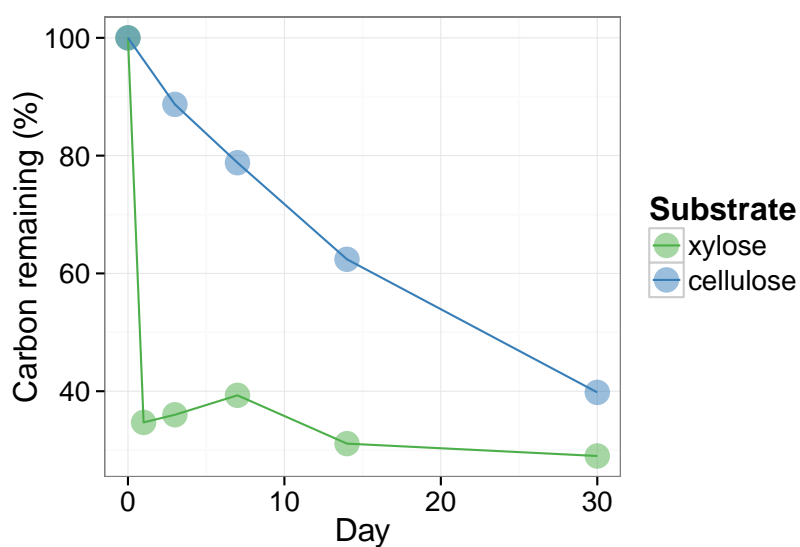


**Fig. 5.**  $^{13}\text{C}$ -responder characteristics based on density shift (A) and rank (B). Kernel density estimation of  $^{13}\text{C}$ -responder's density shift in cellulose treatment (blue) and xylose treatment (green) demonstrates degree of labeling for responders for each respective substrate.  $^{13}\text{C}$ -responders in rank abundance are labeled by substrate (cellulose, blue; xylose, green). Ticks at top indicate location of  $^{13}\text{C}$ -cylose responders in bulk community. Ticks at bottom indicate location of  $^{13}\text{C}$ -cellulose responders in bulk community. OTU rank was assessed from day 1 bulk samples.

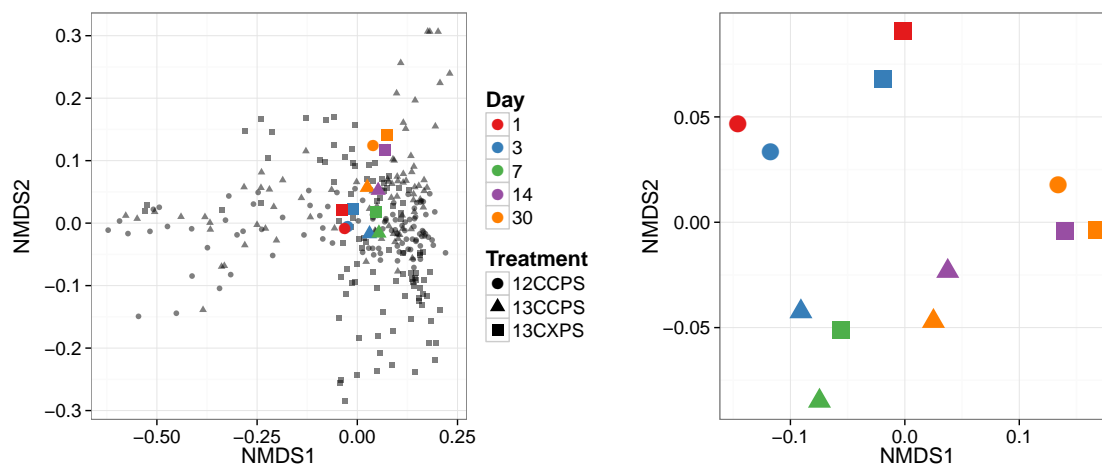
**Supplemental Figures and Tables**



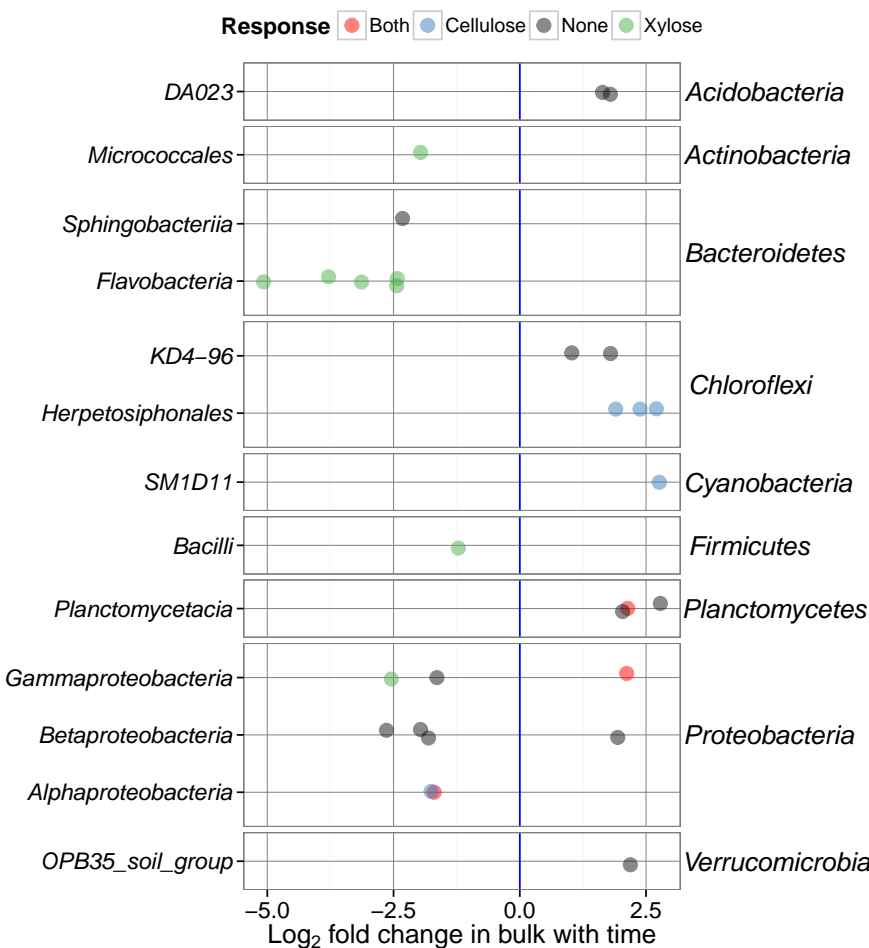
**Fig. S1.** The experimental design. A carbon mixture, in addition to inorganic salts and amino acids (not shown here), was added to each soil microcosm where the only difference between treatments is the <sup>13</sup>C-labeled isotope (in red). At days 1, 3, 7, 14, and 30 replicate microcosms were destructively harvested for downstream molecular applications. Bulk DNA from each treatment and time point ( $n = 14$ ) was CsCl density separated by centrifuged and fractionated (orange tubes wherein each arrow represents a fraction from the density gradient). Fractions were 16S gene sequenced using next generation sequencing technology.



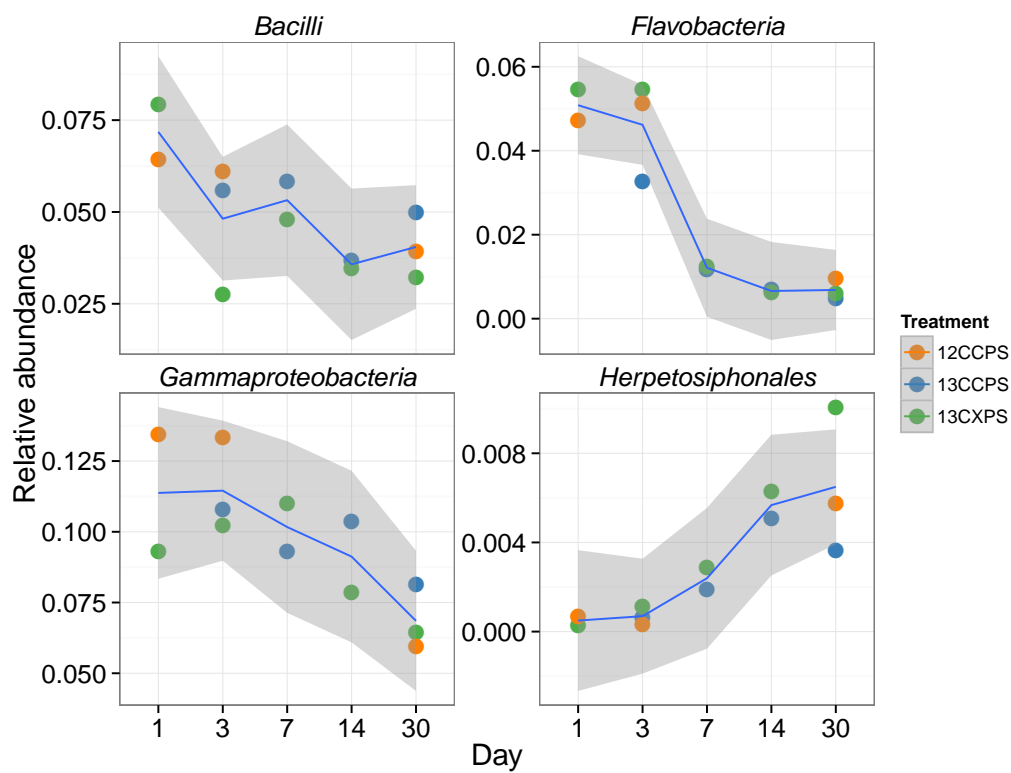
**Fig. S2.** Percentage of added <sup>13</sup>C remaining in soil over time.



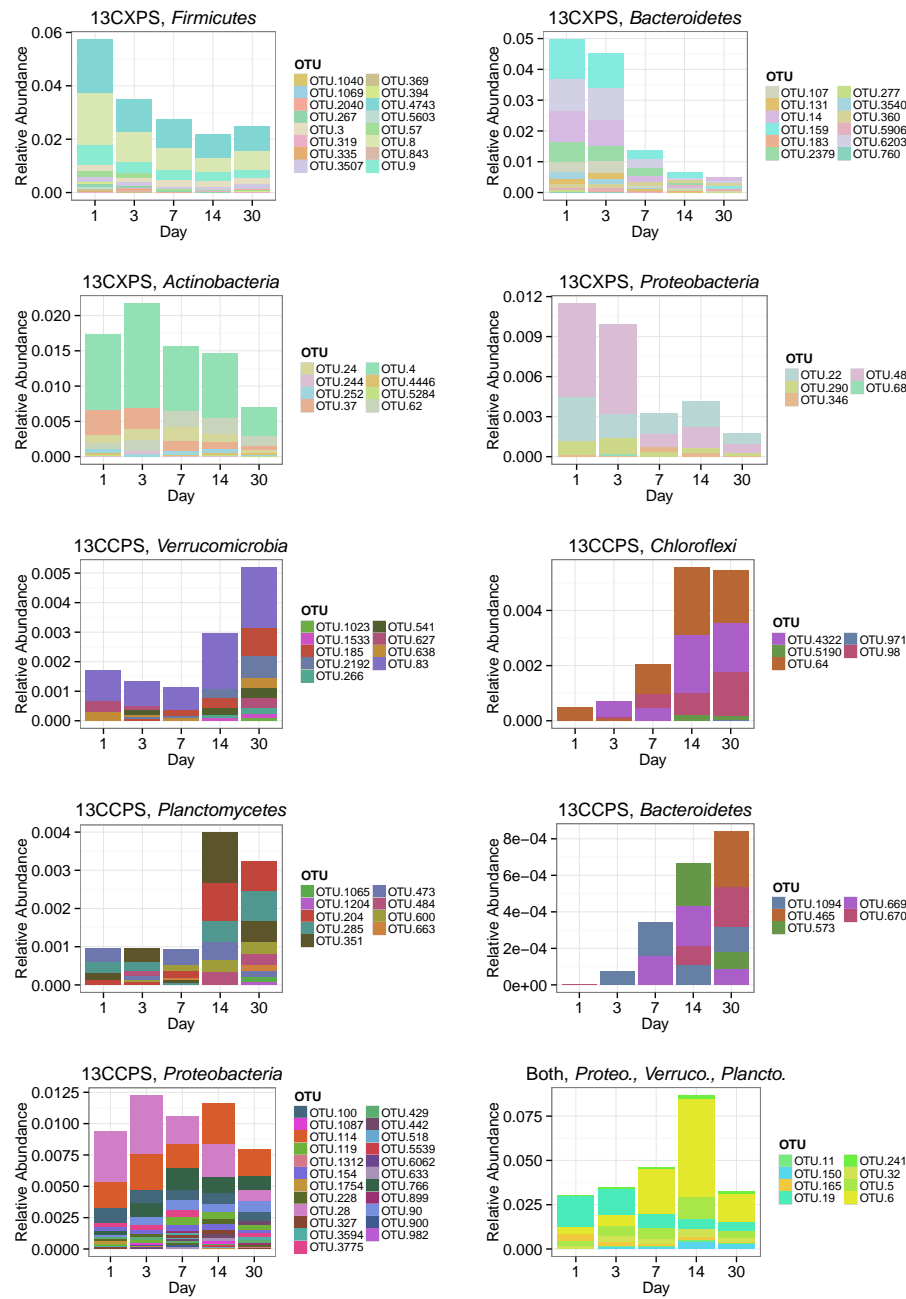
**Fig. S3.** Ordination of bulk gradient fraction phylogenetic profiles.



**Fig. S4.** Fold change time<sup>-1</sup> for OTUs that changed significantly in abundance over time. One panel per phylum (phyla indicated on the right). Taxonomic class indicated on the left.



**Fig. S5.** Relative abundance versus day for classes that changed significantly in relative abundance with time.

**Fig. S6.** Sum of bulk abundances with selected phylum for responder OTUs.

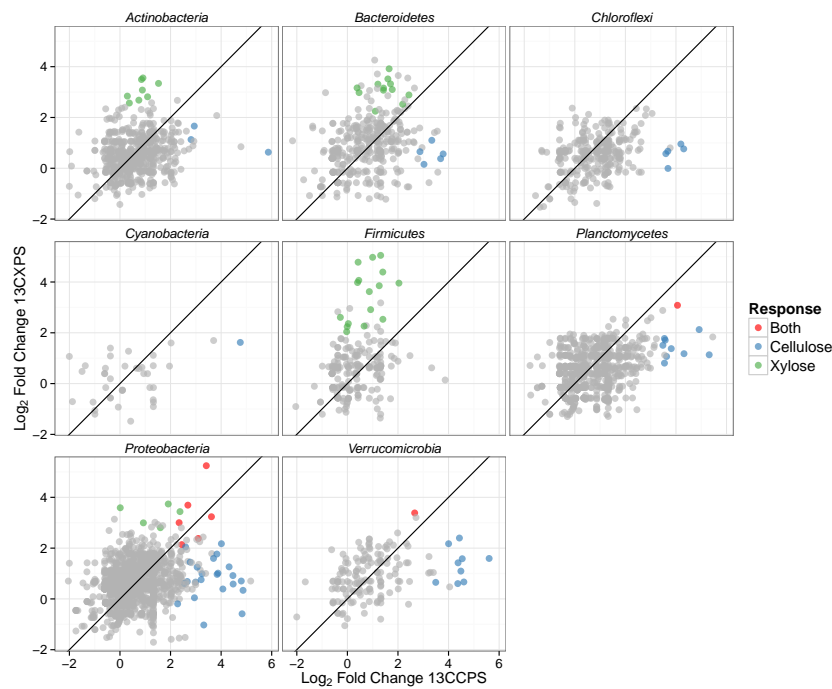


**Fig. S7.** Maximum log<sub>2</sub> fold change in response to labeled substrate incorporation for each substrate and all OTUs that pass sparsity filtering in both substrate analyses. Points colored by response. Line has slope of 1 with intercept at the origin. OTUs falling in the top-right quadrant responded to both substrates while those in the top-left and bottom-right responded to <sup>13</sup>C-xylose and <sup>13</sup>C-cellulose, respectively.

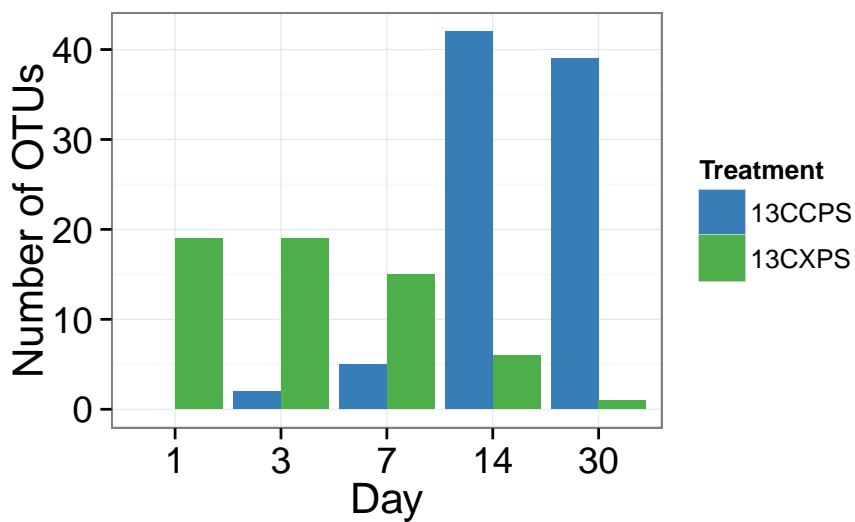


**Fig. S8.** Counts of responders to each isotopically labeled substrate (cellulose and xylose) over time.

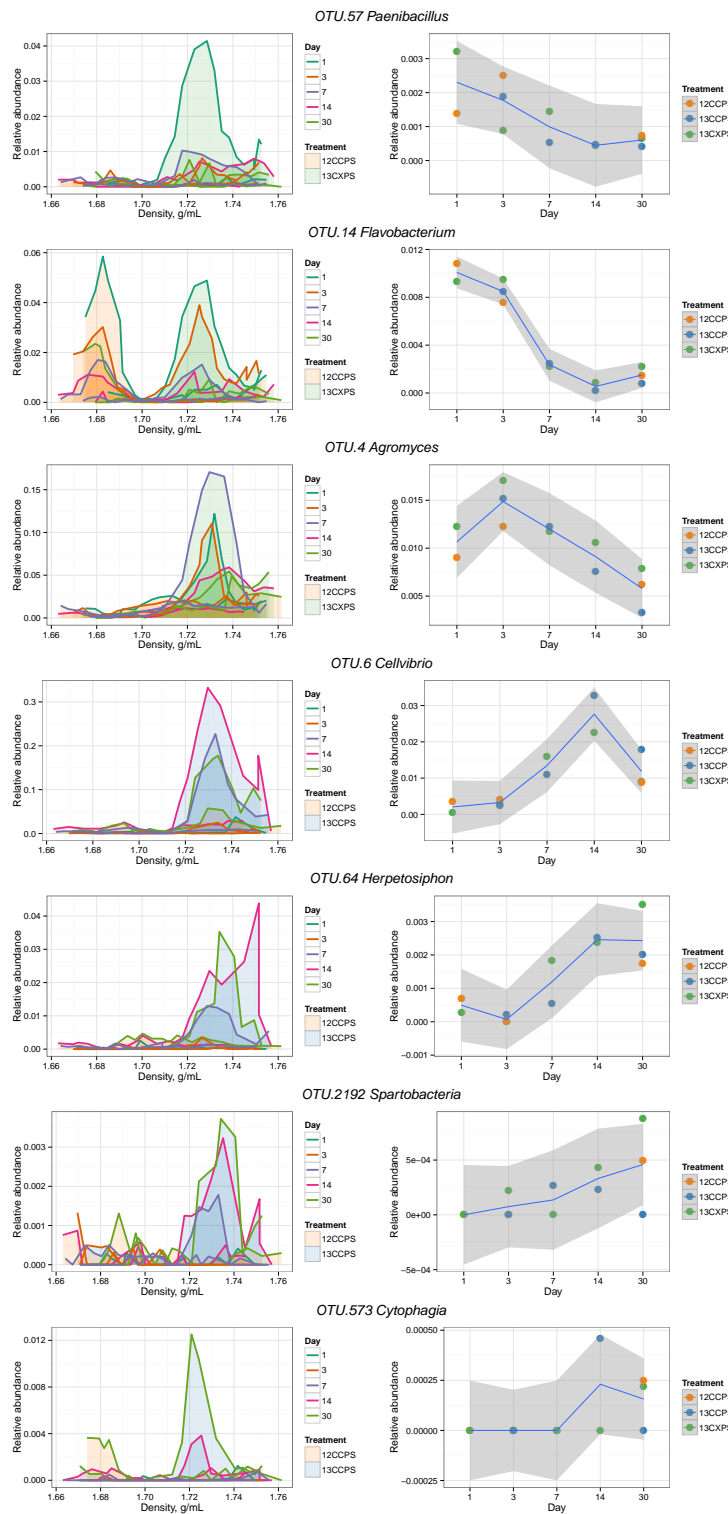


**Fig. S9.** The left column shows DNA-SIP density fraction relative abundances for all gradients for each of the OTUs. Gradient profiles are shaded by treatment where orange represents “control” profiles, blue “<sup>13</sup>C-cellulose”, and green “<sup>13</sup>C-xylose.” The right column shows the abundance of each OTU in non-fractionated DNA (i.e. the DNA that was subsequently fractionated on the density gradient). Enrichment in the heavy end of the gradient in <sup>13</sup>C treatments indicates an OTU has <sup>13</sup>C-labeled DNA that is greater in buoyant density than it would be unlabeled.

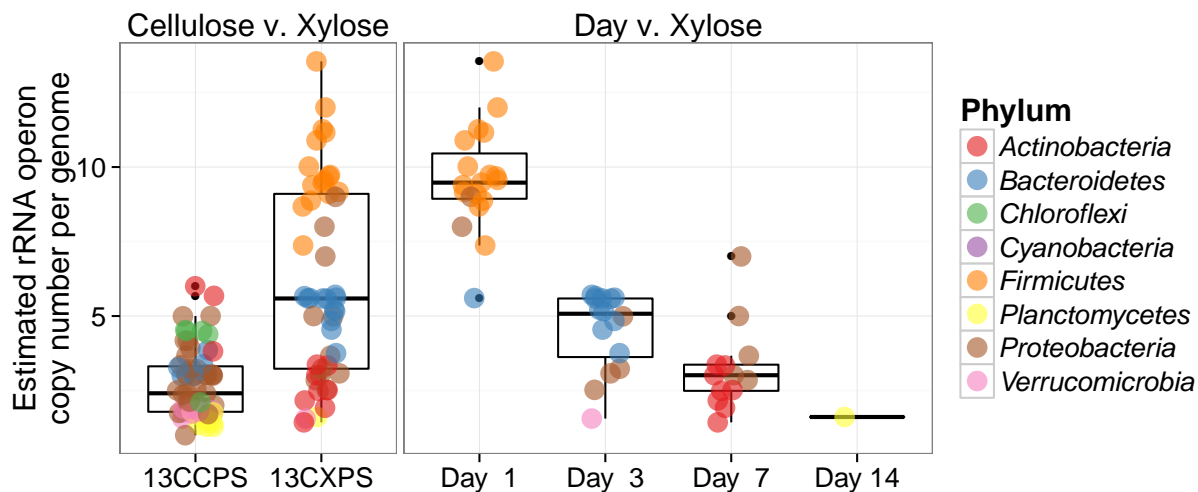


**Fig. S10.** Estimated rRNA operon copy number per genome for  $^{13}\text{C}$  responding OTUs. Panel titles indicate which labeled substrate(s) are depicted.

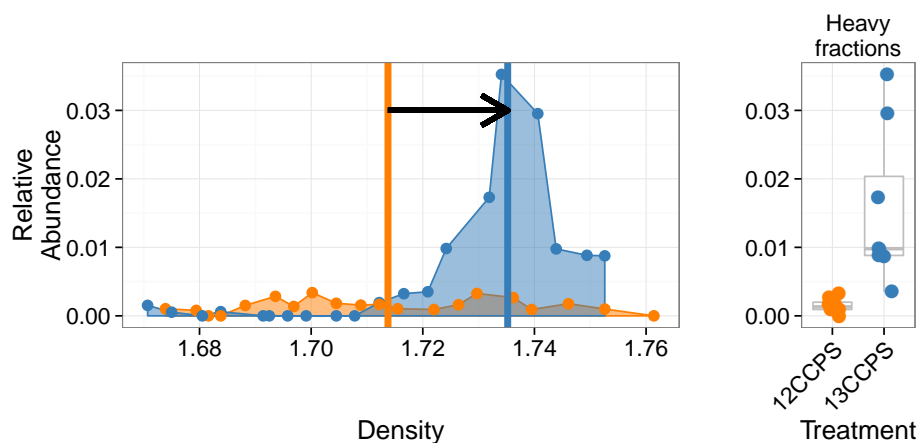


**Fig. S11.** Density profile for a single  $^{13}\text{C}$ -cellulose “responder” OTU in the labeled gradient, blue, and the control gradient, orange. Vertical lines show center of mass for each density profile and arrow denotes the magnitude and direction of the BD shift upon labeling. Panel at right shows relative abundance values in the heavy fractions for each gradient.

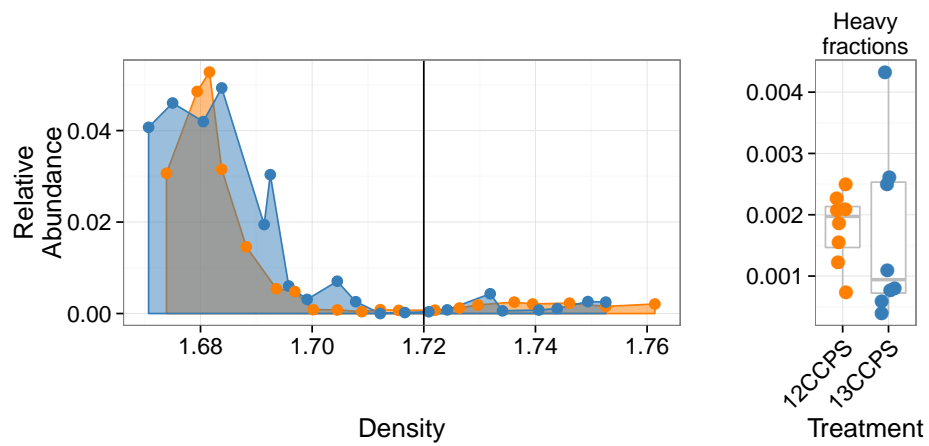


**Fig. S12.** Density profile for a single  $^{13}\text{C}$ -cellulose "non-responder" OTU in the labeled gradient, blue, and the control gradient, orange. Vertical line shows where "heavy" fractions begin as defined in our analysis. Panel at right shows relative abundance values in the heavy fractions for each gradient.

Table S1: <sup>13</sup>C-cellulose responders BLAST against Living Tree Project

OTU ID	Fold change <sup>a</sup>	Day <sup>b</sup>	Top BLAST hits	BLAST %ID	Phylum;Class;Order
OTU.100	2.66	14	<i>Pseudoxanthomonas sacheonensis</i> , <i>Pseudoxanthomonas dokdonensis</i>	100.0	Proteobacteria Gammaproteobacteria Xanthomonadales
OTU.1023	4.61	30	No hits of at least 90% identity	80.54	Verrucomicrobia Spartobacteria Chthoniobacterales
OTU.1065	5.31	14	No hits of at least 90% identity	84.55	Planctomycetes Planctomycetacia Planctomycetales
OTU.1087	4.32	14	<i>Devsia soli</i> , <i>Devsia crocina</i> , <i>Devsia riboflavina</i>	99.09	Proteobacteria Alphaproteobacteria Rhizobiales
OTU.1094	3.69	30	<i>Sporocytophaga myxococcoides</i>	99.55	Bacteroidetes Cytophagia Cytophagales
OTU.11	3.41	14	<i>Stenotrophomonas pavanii</i> , <i>Stenotrophomonas maltophilia</i> , <i>Pseudomonas geniculata</i>	99.54	Proteobacteria Gammaproteobacteria Xanthomonadales
OTU.114	2.78	14	<i>Herbaspirillum sp. SUEMI03</i> , <i>Herbaspirillum sp. SUEMI10</i> , <i>Oxalicibacterium solurbis</i> , <i>Herminiumonas fonticola</i> , <i>Oxalicibacterium horti</i>	100.0	Proteobacteria Betaproteobacteria Burkholderiales
OTU.119	3.31	14	<i>Brevundimonas alba</i>	100.0	Proteobacteria Alphaproteobacteria Caulobacterales
OTU.120	4.76	14	<i>Vampirovibrio chlorellavorus</i>	94.52	Cyanobacteria SM1D11 uncultured-bacterium
OTU.1204	4.32	30	<i>Planctomyces limnophilus</i>	91.78	Planctomycetes Planctomycetacia Planctomycetales
OTU.1312	4.07	30	<i>Paucimonas lemoignei</i>	99.54	Proteobacteria Betaproteobacteria Burkholderiales
OTU.132	2.81	14	<i>Streptomyces spp.</i>	100.0	Actinobacteria Streptomycetales Streptomycetaceae
OTU.150	4.06	14	No hits of at least 90% identity	86.76	Planctomycetes Planctomycetacia Planctomycetales
OTU.1533	3.43	30	No hits of at least 90% identity	82.27	Verrucomicrobia Spartobacteria Chthoniobacterales
OTU.154	3.24	14	<i>Pseudoxanthomonas mexicana</i> , <i>Pseudoxanthomonas japonensis</i>	100.0	Proteobacteria Gammaproteobacteria Xanthomonadales
OTU.165	3.1	14	<i>Rhizobium skieniewicense</i> , <i>Rhizobium vignae</i> , <i>Rhizobium larrymoorei</i> , <i>Rhizobium alkalisolii</i> , <i>Rhizobium galegae</i> , <i>Rhizobium huautlense</i>	100.0	Proteobacteria Alphaproteobacteria Rhizobiales
OTU.1754	4.48	14	<i>Asticcacaulis biprosthecium</i> , <i>Asticcacaulis benevestitus</i>	96.8	Proteobacteria Alphaproteobacteria Caulobacterales
OTU.185	4.37	14	No hits of at least 90% identity	85.14	Verrucomicrobia Spartobacteria Chthoniobacterales
OTU.19	2.44	14	<i>Rhizobium alamii</i> , <i>Rhizobium mesosinicum</i> , <i>Rhizobium mongolense</i> , <i>Arthrobacter viscosus</i> , <i>Rhizobium sullae</i> , <i>Rhizobium yanglingense</i> , <i>Rhizobium loessense</i>	99.54	Proteobacteria Alphaproteobacteria Rhizobiales
OTU.204	3.81	14	No hits of at least 90% identity	nan	Planctomycetes Planctomycetacia Planctomycetales

Table S1 – continued from previous page

OTU ID	Fold change	Day	Top BLAST hits	BLAST %ID	Phylum;Class;Order
OTU.2192	3.49	30	No hits of at least 90% identity	83.56	Verrucomicrobia Spartobacteria Chthoniobacterales
OTU.228	2.54	30	<i>Sorangium cellulosum</i>	98.17	Proteobacteria Deltaproteobacteria Myxococcales
OTU.241	2.66	14	No hits of at least 90% identity	87.73	Verrucomicrobia Spartobacteria Chthoniobacterales
OTU.257	2.94	14	<i>Lentzea waywayandensis</i> , <i>Lentzea flaviverrucosa</i>	100.0	Actinobacteria Pseudonocardiales Pseudonocardiaceae
OTU.266	4.54	30	No hits of at least 90% identity	83.64	Verrucomicrobia Spartobacteria Chthoniobacterales
OTU.28	2.59	14	<i>Rhizobium giardinii</i> , <i>Rhizobium tubonense</i> , <i>Rhizobium tibeticum</i> , <i>Rhizobium mesoamericanum CCGE 501</i> , <i>Rhizobium herbae</i> , <i>Rhizobium endophyticum</i>	99.54	Proteobacteria Alphaproteobacteria Rhizobiales
OTU.285	3.55	30	<i>Blastopirellula marina</i>	90.87	Planctomycetes Planctomycetacia Planctomycetales
OTU.32	2.34	3	<i>Sandaracinus amyloyticus</i>	94.98	Proteobacteria Deltaproteobacteria Myxococcales
OTU.327	2.99	14	<i>Asticcacaulis biprosthecum</i> , <i>Asticcacaulis benevestitus</i>	98.63	Proteobacteria Alphaproteobacteria Caulobacterales
OTU.351	3.54	14	<i>Pirellula staleyi DSM 6068</i>	91.86	Planctomycetes Planctomycetacia Planctomycetales
OTU.3594	3.83	30	<i>Chondromyces robustus</i>	90.41	Proteobacteria Deltaproteobacteria Myxococcales
OTU.3775	3.88	14	<i>Devosia glacialis</i> , <i>Devosia chinhatensis</i> , <i>Devosia geojensis</i> , <i>Devosia yakushimensis</i>	98.63	Proteobacteria Alphaproteobacteria Rhizobiales
OTU.429	3.7	30	<i>Devosia limi</i> , <i>Devosia psychrophila</i>	97.72	Proteobacteria Alphaproteobacteria Rhizobiales
OTU.4322	4.19	14	No hits of at least 90% identity	89.14	Chloroflexi Herpetosiphonales Herpetosiphonaceae
OTU.442	3.05	30	<i>Chondromyces robustus</i>	92.24	Proteobacteria Deltaproteobacteria Myxococcales
OTU.465	3.79	30	<i>Ohtaekwangia kribbensis</i>	92.73	Bacteroidetes Cytophagia Cytophagales
OTU.473	3.58	14	<i>Pirellula staleyi DSM 6068</i>	90.91	Planctomycetes Planctomycetacia Planctomycetales
OTU.484	4.92	14	No hits of at least 90% identity	89.09	Planctomycetes Planctomycetacia Planctomycetales
OTU.5	2.69	14	<i>Delftia tsuruhatensis</i> , <i>Delftia lacustris</i>	100.0	Proteobacteria Betaproteobacteria Burkholderiales
OTU.518	4.8	14	<i>Hydrogenophaga intermedia</i>	100.0	Proteobacteria Betaproteobacteria Burkholderiales
OTU.5190	3.6	30	No hits of at least 90% identity	88.13	Chloroflexi Herpetosiphonales Herpetosiphonaceae
OTU.541	4.49	30	No hits of at least 90% identity	84.23	Verrucomicrobia Spartobacteria Chthoniobacterales
OTU.5539	4.01	14	<i>Devosia subaequoris</i>	98.17	Proteobacteria Alphaproteobacteria Rhizobiales

Table S1 – continued from previous page

OTU ID	Fold change	Day	Top BLAST hits	BLAST %ID	Phylum;Class;Order
OTU.573	3.03	30	<i>Adhaeribacter aerophilus</i>	92.76	<i>Bacteroidetes Cytophagia Cytophagales</i>
OTU.6	3.62	7	<i>Cellvibrio fulvus</i>	100.0	<i>Proteobacteria Gammaproteobacteria Pseudomonadales</i>
OTU.600	3.48	30	No hits of at least 90% identity	80.37	<i>Planctomycetes Planctomycetacia Planctomycetales</i>
OTU.6062	4.83	30	<i>Dokdonella sp. DC-3, Luteibacter rhizovicinus</i>	97.26	<i>Proteobacteria Gammaproteobacteria Xanthomonadales</i>
OTU.627	4.43	14	<i>Verrucomicrobiaceae bacterium DC2a-G7</i>	100.0	<i>Verrucomicrobia Verrucomicrobiae Verrucomicrobiales</i>
OTU.633	3.84	30	No hits of at least 90% identity	89.5	<i>Proteobacteria Deltaproteobacteria Myxococcales</i>
OTU.638	4.0	30	<i>Luteolibacter sp. CCTCC AB 2010415, Luteolibacter algae</i>	93.61	<i>Verrucomicrobia Verrucomicrobiae Verrucomicrobiales</i>
OTU.64	4.31	14	No hits of at least 90% identity	89.5	<i>Chloroflexi Herpetosiphonales Herpetosiphonaceae</i>
OTU.663	3.63	30	<i>Pirellula staleyi DSM 6068</i>	90.87	<i>Planctomycetes Planctomycetacia Planctomycetales</i>
OTU.669	3.34	30	<i>Ohtaekwangia koreensis</i>	92.69	<i>Bacteroidetes Cytophagia Cytophagales</i>
OTU.670	2.87	30	<i>Adhaeribacter aerophilus</i>	91.78	<i>Bacteroidetes Cytophagia Cytophagales</i>
OTU.766	3.21	14	<i>Devosia insulae</i>	99.54	<i>Proteobacteria Alphaproteobacteria Rhizobiales</i>
OTU.83	5.61	14	<i>Luteolibacter sp. CCTCC AB 2010415</i>	97.72	<i>Verrucomicrobia Verrucomicrobiae Verrucomicrobiales</i>
OTU.862	5.87	14	<i>Allokutzneria albata</i>	100.0	<i>Actinobacteria Pseudonocardiales Pseudonocardiaceae</i>
OTU.899	2.28	30	<i>Enhygromyxa salina</i>	97.72	<i>Proteobacteria Deltaproteobacteria Myxococcales</i>
OTU.90	2.94	14	<i>Sphingopyxis panaciterrae, Sphingopyxis chilensis, Sphingopyxis sp. BZ30, Sphingomonas sp.</i>	100.0	<i>Proteobacteria Alphaproteobacteria Sphingomonadales</i>
OTU.900	4.87	14	<i>Brevundimonas vesicularis, Brevundimonas nasdae</i>	100.0	<i>Proteobacteria Alphaproteobacteria Caulobacterales</i>
OTU.971	3.68	30	No hits of at least 90% identity	78.57	<i>Chloroflexi Anaerolineae Anaerolineales</i>
OTU.98	3.68	14	No hits of at least 90% identity	88.18	<i>Chloroflexi Herpetosiphonales Herpetosiphonaceae</i>
OTU.982	4.47	14	<i>Devosia neptuniae</i>	100.0	<i>Proteobacteria Alphaproteobacteria Rhizobiales</i>

<sup>a</sup> Maximum observed  $\log_2$  of fold change.<sup>b</sup> Day of maximum fold change.

Table S2:  $^{13}\text{C}$ -xylose responders BLAST against Living Tree Project

OTU ID	Fold change <sup>a</sup>	Day <sup>b</sup>	Top BLAST hits	BLAST %ID	Phylum;Class;Order
OTU.1040	4.78	1	<i>Paenibacillus daejeonensis</i>	100.0	<i>Firmicutes Bacilli Bacillales</i>
OTU.1069	3.85	1	<i>Paenibacillus terrigena</i>	100.0	<i>Firmicutes Bacilli Bacillales</i>
OTU.107	2.25	3	<i>Flavobacterium sp. 15C3</i> , <i>Flavobacterium banpakuense</i>	99.54	<i>Bacteroidetes Flavobacteria Flavobacteriales</i>
OTU.11	5.25	7	<i>Stenotrophomonas pavanii</i> , <i>Stenotrophomonas maltophilia</i> , <i>Pseudomonas geniculata</i>	99.54	<i>Proteobacteria Gammaproteobacteria Xanthomonadales</i>
OTU.131	3.07	3	<i>Flavobacterium fluvii</i> , <i>Flavobacterium bacterium HMD1033</i> , <i>Flavobacterium sp. HMD1001</i>	100.0	<i>Bacteroidetes Flavobacteria Flavobacteriales</i>
OTU.14	3.92	3	<i>Flavobacterium oncorhynchi</i> , <i>Flavobacterium glycines</i> , <i>Flavobacterium succinicans</i>	99.09	<i>Bacteroidetes Flavobacteria Flavobacteriales</i>
OTU.150	3.08	14	No hits of at least 90% identity	86.76	<i>Planctomycetes Planctomycetacia Planctomycetales</i>
OTU.159	3.16	3	<i>Flavobacterium hibernum</i>	98.17	<i>Bacteroidetes Flavobacteria Flavobacteriales</i>
OTU.165	2.38	3	<i>Rhizobium skieniewicense</i> , <i>Rhizobium vignae</i> , <i>Rhizobium larrymoorei</i> , <i>Rhizobium alkalisolii</i> , <i>Rhizobium galegae</i> , <i>Rhizobium huautlense</i>	100.0	<i>Proteobacteria Alphaproteobacteria Rhizobiales</i>
OTU.183	3.31	3	No hits of at least 90% identity	89.5	<i>Bacteroidetes Sphingobacteriia Sphingobacteriales</i>
OTU.19	2.14	7	<i>Rhizobium alamii</i> , <i>Rhizobium mesosinicum</i> , <i>Rhizobium mongolense</i> , <i>Arthrobacter viscosus</i> , <i>Rhizobium sullae</i> , <i>Rhizobium yanglingense</i> , <i>Rhizobium loessense</i>	99.54	<i>Proteobacteria Alphaproteobacteria Rhizobiales</i>
OTU.2040	2.91	1	<i>Paenibacillus pectinilyticus</i>	100.0	<i>Firmicutes Bacilli Bacillales</i>
OTU.22	2.8	7	<i>Paracoccus sp. NB88</i>	99.09	<i>Proteobacteria Alphaproteobacteria Rhodobacterales</i>
OTU.2379	3.1	3	<i>Flavobacterium pectinovorum</i> , <i>Flavobacterium sp. CS100</i>	97.72	<i>Bacteroidetes Flavobacteria Flavobacteriales</i>
OTU.24	2.81	7	<i>Cellulomonas aerilata</i> , <i>Cellulomonas humilata</i> , <i>Cellulomonas terrae</i> , <i>Cellulomonas soli</i> , <i>Cellulomonas xylinilytica</i>	100.0	<i>Actinobacteria Micrococcales Cellulomonadaceae</i>
OTU.241	3.38	3	No hits of at least 90% identity	87.73	<i>Verrucomicrobia Spartobacteria Chthoniobacterales</i>
OTU.244	3.08	7	<i>Cellulosimicrobium funkei</i> , <i>Cellulosimicrobium terreum</i>	100.0	<i>Actinobacteria Micrococcales Promicromonosporaceae</i>
OTU.252	3.34	7	<i>Promicromonospora thailandica</i>	100.0	<i>Actinobacteria Micrococcales Promicromonosporaceae</i>
OTU.267	4.97	1	<i>Paenibacillus pabuli</i> , <i>Paenibacillus tundrae</i> , <i>Paenibacillus taichungensis</i> , <i>Paenibacillus xylohexedens</i> , <i>Paenibacillus xylinilyticus</i>	100.0	<i>Firmicutes Bacilli Bacillales</i>
OTU.277	3.52	3	<i>Solibius ginsengiterrae</i>	95.43	<i>Bacteroidetes Sphingobacteriia Sphingobacteriales</i>

Table S2 – continued from previous page

OTU ID	Fold change	Day	Top BLAST hits	BLAST %ID	Phylum;Class;Order
OTU.290	3.59	1	<i>Pantoea spp.</i> , <i>Klugvera spp.</i> , <i>Klebsiella spp.</i> , <i>Erwinia spp.</i> , <i>Enterobacter spp.</i> , <i>Buttiauxella spp.</i>	100.0	Proteobacteria Gammaproteobacteria Enterobacterales
OTU.3	2.61	1	[ <i>Brevibacterium</i> ] <i>frigoritolerans</i> , <i>Bacillus sp.</i> LMG 20238, <i>Bacillus coahuilensis</i> m4-4, <i>Bacillus simplex</i>	100.0	Firmicutes Bacilli Bacillales
OTU.319	3.98	1	<i>Paenibacillus xinjiangensis</i>	97.25	Firmicutes Bacilli Bacillales
OTU.32	3.0	3	<i>Sandaracinus amyloyticus</i>	94.98	Proteobacteria Deltaproteobacteria Myxococcales
OTU.335	2.53	1	<i>Paenibacillus thailandensis</i>	98.17	Firmicutes Bacilli Bacillales
OTU.346	3.44	3	<i>Pseudoduganella violaceinigra</i>	99.54	Proteobacteria Betaproteobacteria Burkholderiales
OTU.3507	2.36	1	<i>Bacillus spp.</i>	98.63	Firmicutes Bacilli Bacillales
OTU.3540	2.52	3	<i>Flavobacterium terrigena</i>	99.54	Bacteroidetes Flavobacteria Flavobacterales
OTU.360	2.98	3	<i>Flavisolibacter ginsengisoli</i>	95.0	Bacteroidetes Sphingobacteriia Sphingobacterales
OTU.369	5.05	1	<i>Paenibacillus sp.</i> D75, <i>Paenibacillus glycansilyticus</i>	100.0	Firmicutes Bacilli Bacillales
OTU.37	2.68	7	<i>Phycicola gilvus</i> , <i>Microterricola viridarii</i> , <i>Frigeribacterium faeni</i> , <i>Frondihabitans sp.</i> RS-15, <i>Frondihabitans australicus</i>	100.0	Actinobacteria Micrococcales Microbacteriaceae
OTU.394	4.06	1	<i>Paenibacillus pocheonensis</i>	100.0	Firmicutes Bacilli Bacillales
OTU.4	2.84	7	<i>Agromyces ramosus</i>	100.0	Actinobacteria Micrococcales Microbacteriaceae
OTU.4446	3.49	7	<i>Catenuloplanes niger</i> , <i>Catenuloplanes castaneus</i> , <i>Catenuloplanes atrovinosus</i> , <i>Catenuloplanes crispus</i> , <i>Catenuloplanes nepalensis</i> , <i>Catenuloplanes japonicus</i>	97.72	Actinobacteria Frankiales Nakamurellaceae
OTU.4743	2.24	1	<i>Lysinibacillus fusiformis</i> , <i>Lysinibacillus sphaericus</i>	99.09	Firmicutes Bacilli Bacillales
OTU.48	2.99	1	<i>Aeromonas spp.</i>	100.0	Proteobacteria Gammaproteobacteria aaa34a10
OTU.5	3.69	7	<i>Delftia tsuruhatensis</i> , <i>Delftia lacustris</i>	100.0	Proteobacteria Betaproteobacteria Burkholderiales
OTU.5284	3.56	7	<i>Isoptericola nanjingensis</i> , <i>Isoptericola hypogaeus</i> , <i>Isoptericola variabilis</i>	98.63	Actinobacteria Micrococcales Promicromonosporaceae
OTU.5603	3.96	1	<i>Paenibacillus uliginis</i>	100.0	Firmicutes Bacilli Bacillales
OTU.57	4.39	1	<i>Paenibacillus castaneae</i>	98.62	Firmicutes Bacilli Bacillales
OTU.5906	3.16	3	<i>Terrimonas sp.</i> M-8	96.8	Bacteroidetes Sphingobacteriia Sphingobacterales
OTU.6	3.24	3	<i>Cellvibrio fulvus</i>	100.0	Proteobacteria Gammaproteobacteria Pseudomonadales
OTU.62	2.57	7	<i>Nakamurella flava</i>	100.0	Actinobacteria Frankiales Nakamurellaceae

Table S2 – continued from previous page

OTU ID	Fold change	Day	Top BLAST hits	BLAST %ID	Phylum;Class;Order
OTU.6203	3.32	3	<i>Flavobacterium granuli</i> , <i>Flavobacterium glaciei</i>	100.0	<i>Bacteroidetes Flavobacteria Flavobacteriales</i>
OTU.68	3.74	7	<i>Shigella flexneri</i> , <i>Escherichia fergusonii</i> , <i>Escherichia coli</i> , <i>Shigella sonnei</i>	100.0	<i>Proteobacteria Gammaproteobacteria Enterobacteriales</i>
OTU.760	2.89	3	<i>Dyadobacter hamtensis</i>	98.63	<i>Bacteroidetes Cytophagia Cytophagales</i>
OTU.8	2.26	1	<i>Bacillus niaci</i>	100.0	<i>Firmicutes Bacilli Bacillales</i>
OTU.843	3.62	1	<i>Paenibacillus agaragedens</i>	100.0	<i>Firmicutes Bacilli Bacillales</i>
OTU.9	2.04	1	<i>Bacillus megaterium</i> , <i>Bacillus flexus</i>	100.0	<i>Firmicutes Bacilli Bacillales</i>

<sup>a</sup> Maximum observed  $\log_2$  of fold change.<sup>b</sup> Day of maximum fold change.